AF-85-01

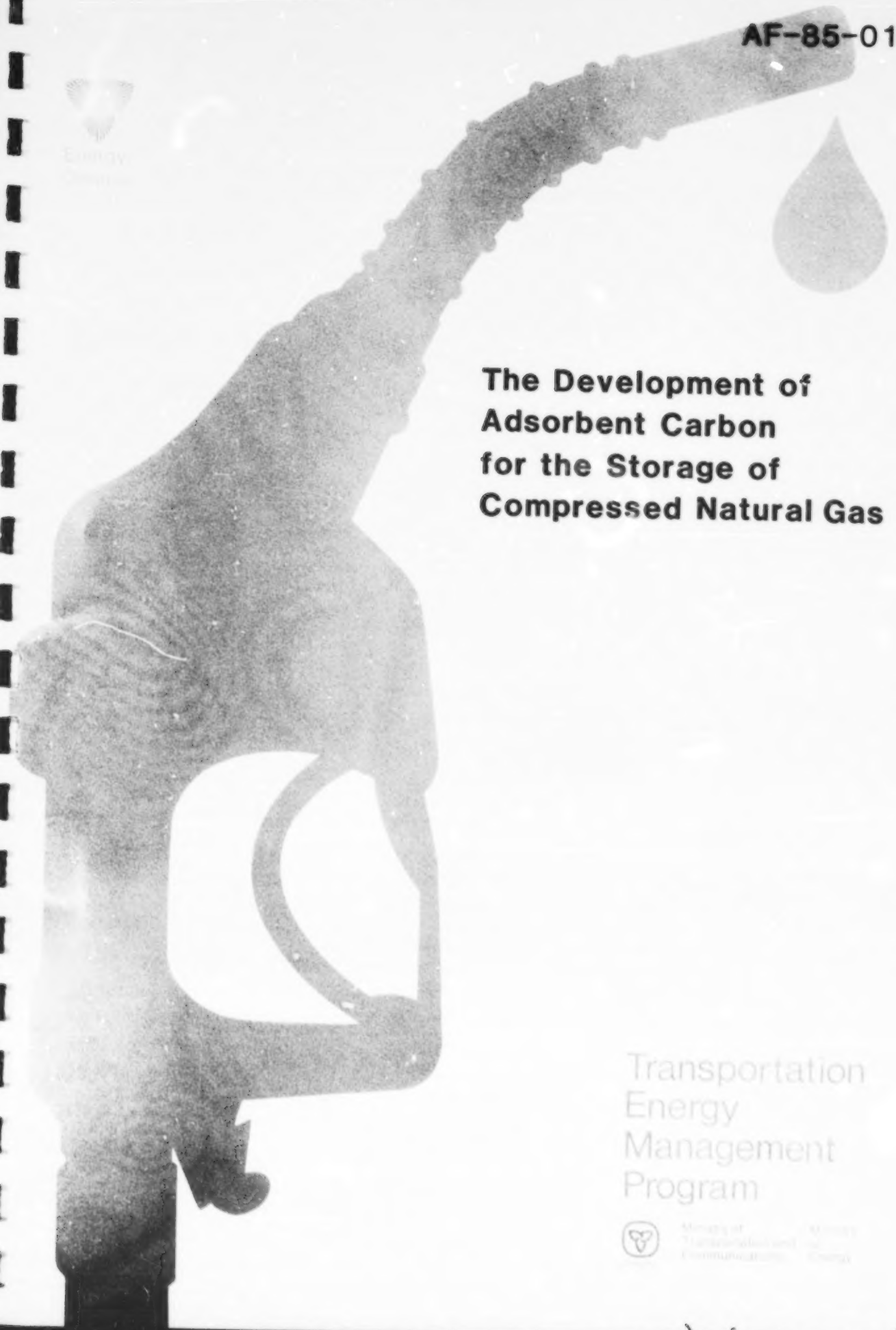

The Development of Adsorbent Carbon for the Storage of Compressed Natural Gas

Transportation Energy Management Program

Ministry of Transportation and Communications

AF-85-01

The Development of Adsorbent Carbon for the Storage of Compressed Natural Gas

S.S. Barton
J.A. Holland
D.F. Quinn
Department of Chemistry and Chemical Engineering
Royal Military College of Canada
Kingston, Ontario

Published by:
Automotive Technology and Systems Office
Ontario Ministry of Transportation and Communications
Hon. George McCague, Minister
H.F. Gilbert, Deputy Minister

Ontario Ministry of Energy
Hon. Michael Harris, Minister
D.M. Allan, Deputy Minister

Published without prejudice
as to the application of the findings.
Crown copyright reserved; however, this
document may be reproduced for non-commercial
purposes with attribution to the Ministry.

For additional copies, write:
The Editor, Technical Publications
Ministry of Transportation and Communications
1201 Wilson Avenue
Downsview, Ontario
Canada M3M 1J8

May 1985

Technical Report Documentation Page

MTC Report Number: AF-85-01	ISBN Number:	Other Document Number:	Date: June 1985

Title: The Development of Adsorbent Carbon for the Storage of Compressed Natural Gas

Authors (name, title and/or organization):
S.S Barton, Royal Military College of Canada
J.A. Holland, Royal Military College of Canada
D.F. Quinn, Royal Military College of Canada

Published by:
Automotive Technology and Systems Office
Transportation Technology and Energy Branch, MTC
and
Ontario Ministry of Energy

Client Group:

Participating Agencies:
Royal Military College of Canada
Ontario Ministry of Transportation and Communications
Ontario Ministry of Energy

Abstract:
This report is the third in a series dealing with the development of adsorbents for the storage of compressed natural gas on board vehicles. A previously identified carbon product, based on Saran polymer, has now been prepared in kilogram quantities. To minimize void space, monolithic pieces have been made in the form of discs so as to fill a container. The material has been repeatedly filled with methane under pressure and then emptied to test thermal effects, durability under cycling, etc. Additional work has also been done to improve the basic properties of the material by steam activation.

Key Words: CNG storage, adsorption, carbon, methane

Comments:

Distribution: by request

Copyright Status: Crown copyright

ABSTRACT

Saran carbon has been investigated as an adsorbent for methane at pressures up to 10.34 MPa (1500 psia). Two separate studies were conducted.

The first was to produce Saran carbon in appropriately shaped pieces to fill a 1 L storage vessel with as little void volume as possible. Methane storage was then measured and the carbon sample subjected to repeated fill-empty cycles at pressures to 3.445 MPa (500 psia).

No reduction in storage capacity with cycling was found, and there was no observable deterioration of the Saran carbon samples. Gas densities achieved so far at 3.445 MPa (500 psia) are 92 g/L (139 scf/ft^3), which is significantly greater than has been reported to date for any adsorbent at these pressures and ambient temperature.

The second study was to activate Saran carbon in an attempt to increase its adsorption capacity for methane. Activation was carried out with steam and heat treatment. On a mass of adsorbent basis, adsorption of methane is increased considerably with steam activation. From the more practical volume of adsorbent standpoint, however, little or no increase in adsorptive capacity is found. This is due principally to the production of macropore in the carbon.

Heat treatment at temperatures to 1100°C did not alter the properties of Saran carbon prepared at 700°C.

TABLE OF CONTENTS

	PAGE
ABSTRACT	ii
FOREWORD	vi
ACKNOWLEDGEMENTS	vii
1/ INTRODUCTION	1
2/ PREPARATION FOR TESTING	4
2.1/ Cycling.	4
2.2/ Preparation of Saran Carbon Testing.	4
3/ CYCLING TESTS	8
4/ ACTIVATION OF SARAN CARBON	11
4.1/ Steam Activation	11
4.1.1/ Methane Adsorption.	14
4.1.2/ Conclusion on Steam Activation.	17
4.2/ Heat Treatment Activation.	17
5/ REFERENCES	19

LIST OF TABLES

PAGE

1/ IUPAC Classification of Pores by Size. 21
2/ Density Definitions. 21
3/ Volume Utilization 22
4/ Density Volume Relationships 23
5/ Cycling Test Results 24
6/ Predicted Methane Storage. 25
7/ Summary of Cycle Tests 26
8/ Steam-Activated Saran Carbons -- Mercury Porosimetry 27
9/ Steam-Activated Saran Carbons -- Surface Area (m^2/g) 28
10/ Steam-Activated Saran Carbons -- Micropore and Macropore Volumes. 29
11/ Steam-Activated Saran Carbons -- Methane Micropore Densities (Dubinin). 30
12/ Steam-Activated Saran Carbons -- Methane Micropore Densities (Langmuir) 31
13/ Heat Treatment -- Saran Carbons. 32

LIST OF FIGURES

	PAGE
1/ One-Litre Sample Storage Vessel.	33
2/ Cycle Test Apparatus	34
3/ Compression of Saran Polymer	35
4/ Saran Carbon -- Percent of Methane Stored Relative to Saturation at 25°C and 2.067 MPa (300 psia) vs. Time	36
5/ Temperature Transitions During Filling and Emptying Saran Carbon with Methane.	37
6/ Methane Stored at 2.067 MPa (300 psia) vs. Percent Volume as Micropore	38
7/ Densities -- Steam-Activated Saran Carbon.	39
8/ Mercury Porosimetry -- Steam-Activated Saran Carbon.	40
9/ Mercury Porosimetry -- Steam-Activated Saran Carbon Pellets. .	41
10/ Surface Areas -- Steam-Activated Saran Carbon.	42
11/ Methane Surface Areas -- Steam-Activated Saran Carbon.	43
12/ Macropore Volume -- Steam-Activated Saran Carbon	44
13/ Micropore Volume -- Steam-Activated Saran Carbon	45
14/ Micropore Volume per Millilitre Total Volume-- Steam-Activated Saran Carbon	46
15/ Methane Adsorption Isotherms, 25°C -- Steam-Activated Saran Carbon	47
16/ Methane Adsorption -- Steam-Activated Saran Carbon Pellets . .	48
17/ Methane Adsorption, 25°C -- Steam-Activated Saran Carbon . . .	49
18/ Methane Adsorbed per Unit Volume Carbon -- Steam-Activated Saran Carbon	50
19/ Methane Adsorbed per Millilitre of Micropore -- Steam-Activated Saran Carbon	51
20/ Dubinin Plots -- Steam-Activated Saran Carbon.	52
21/ Saturation Densities -- Adsorbed Methane, 25°C	53
22/ Degree of Saturation, Calculated from Dubinin Plots	54
23/ Langmuir Plots -- Methane Isotherms, 25°C.	55
24/ Degree of Saturation, Calculated from Langmuir Plots	56
25/ Mercury Porosimetry -- Heat-Treated Saran Carbons.	57
26/ Methane Adsorption -- Heat-Treated Saran Carbons	58

FOREWORD

The project has been carried out as part of the Ontario government's Transportation Energy Management Program (TEMP), jointly managed by the Ministry of Transportation and Communications and the Ministry of Energy. The TEMP mandate is to reduce Ontario's dependence on conventional petroleum-based fuels, and accordingly, TEMP has promoted research on a number of alternative fuels.

Natural gas is abundant in Canada, and it is an alternative fuel that can be used satisfactorily in suitably modified engines. However, present techniques for using natural gas as an automotive fuel rely mainly on its storage on board vehicles as a compressed natural gas (CNG) in high pressure steel cylinders. Compared to liquid fuels such as gasoline, the energy densities that can reasonably be achieved are low, and unless large storage volumes are used, vehicle range and consequent utility are reduced. Improved storage techniques, particularly if they enable adequate densities to be achieved at lower pressures, would make CNG more comparable with traditional liquid fuels.

The project described here is the third phase of a program aimed at developing adsorbents capable of retaining natural gas at reasonable densities and lower pressures.

ACKNOWLEDGEMENTS

The authors would like to thank Dr. J.R. Dacey and Dr. M.J.B. Evans of the Royal Military College of Canada and Dr. David Elliott of the Ministry of Transportation and Communications for helpful discussions and suggestions.

Sincere thanks are also extended to Mr. H. Wilson for his technical assistance.

1/ INTRODUCTION

In recent years several studies [1-5], including one by the authors for MTC, have been made in an effort to find a commercially suitable adsorbent for natural gas, so that it can be stored at ambient temperatures and relatively low pressures. For use in an automobile the volume of a storage vessel must be similar to that of a gasoline tank. Presently, in many parts of the world, vehicles are using natural gas as a fuel. It is stored as compressed gas in high pressure cylinders, at 13.78 to 20.67 MPa (2000 to 3000 psi). At 13.78 MPa (2000 psi) and 25°C, the density of methane is 108 g/L (163 scf/ft^3); therefore, to be competitive, an adsorbent system should deliver this amount of methane from the same volume but at a lower pressure. The studies carried out to date have indicated that carbons, in general, are better adsorbents than zeolite-type materials for this application.

Since adsorption of methane is taking place at ambient temperatures, some 100°C greater than its critical temperature (-82.5°C), this adsorption will not involve capillary condensation. Consequently, carbons with large micropore volumes (pores of less than 2 nm diameter) should be effective adsorbents. Macropores (pores > 50 nm diameter) and mesopores (diameters from 2 to 50 nm) (Table 1) [6] should have minimal influence on total adsorption [7].

Apparent or packing density of adsorbents has also been shown by these studies [1-5] to be an important parameter in obtaining a high adsorption per unit volume (Table 2). Table 3 illustrates volume utilization, derived from data given in Reference 1. It should be noted that the values of bulk density quoted for Saran carbon in this reference are significantly lower than those achieved in the present study.

In an empty cylinder, all the volume is available to the compressed gas. When a carbon adsorbent is in the vessel, the vessel can be considered as four distinct parts: the space occupied by the carbon atoms, the micropore volume, the macropore volume, and the void volume. The latter two, for methane at ambient temperatures, can be regarded as the same and should be minimized, since they contribute no more than empty cylinder space. Because the density of adsorbed methane is greater than methane

in the gas phase, and adsorption takes place in the micropores, the micropore volume should be maximized. This can, however, only be done to a limiting extent before the carbon skeletal structure collapses.

From a mass adsorbent consideration, the Amoco-type carbons have been identified as showing the greatest adsorption of methane for all pressures up to about 10.34 MPa (1500 psia) of any carbon reported to date. These carbons have a large micropore volume, but they also have a large macropore volume and, consequently, a low apparent or packing density (~0.3 g/mL). The result of this low density is a good, but not superior, adsorption per unit volume. In comparison, Saran carbons have very little or no macropore volume but have considerable micropore volume and a high apparent density. In the previous report [1], Saran carbon, with an apparent density of 0.70 g/mL and an adsorption of 0.091 g methane per gram carbon at 2.067 MPa (300 psia), adsorbs 63 g methane per litre. The compressed G210 carbon reported by Remick [5], with a packing density of 0.59 g/mL and an adsorption of 0.092 g methane per gram carbon at the same pressure, would adsorb almost 55 g methane per litre.

The thrust of this present study was to scale up the previous investigations from samples of a few grams to kilogram size. To that end, a 1 L storage vessel was made. This was incorporated into an apparatus where the weight of gas in the vessel was measured. Adsorbents were subjected to repeated fill-empty cycles.

Since Saran carbons have the highest bulk density of any microporous carbon known and can be fabricated into specific shapes, any void volume in packing them into a vessel can be minimized and the apparent or packing density maximized.

This report deals with the preparation of Saran carbon samples for the cycling apparatus, and their performance is compared to some other carbons.

Unlike many carbons, Saran carbon, as prepared, is a highly microporous material and, as such, requires no activation to make it an efficient adsorbent [8]. However, activation by carbon dioxide [9] and by steam [10] has been reported as increasing the micropore volume and BET [11]

surface area of Saran carbons. There is also some indication that heat treatment alone of Saran carbon to higher temperatures (>700°C) results in higher adsorptive capacity [12].

High pressure adsorption of methane may be improved if activated Saran carbon is used. To that end, Saran carbon was activated by steam and heat treatment and the resulting carbons characterized by low temperature (77 K), nitrogen adsorption, and mercury intrusion. High pressure methane isotherms at 25°C were also carried out.

2/ PREPARATION FOR TESTING

2.1/ Cycling Apparatus

A vessel of approximately 1 L volume was constructed from 7.62-cm-diameter (3-in.-diameter), Schedule 80, stainless steel pipe. A diagram of this vessel is shown in Figure 1. It was pressure tested hydraulically to 41.35 MPa (6000 psi). The vessel was designed to allow full geometric access to the diameter of the vessel so that it could be packed as efficiently as possible. Figure 2 shows the cycling apparatus incorporating this sample storage vessel. Stainless steel 6.35 mm (0.25 in.) tubing was used throughout, except for the large loops, where 3.175-mm-diameter (0.125-in.-diameter) copper tubing was used. Asco solenoid valves, Type 8262D45, suitable for pressures to 3.445 MPa (500 psi), were used. A Swagelok 7 μm filter was used to prevent any carbon from leaving the sample vessel. Pressures were measured using a Matheson test gauge (63-5613) or a National semiconductor pressure transducer (LS 1460-AS). Weighings were made using a Setra 12000 quartz balance. Temperature changes were measured with an iron-constantan thermocouple and continuously recorded with an Omniscribe recorder.

The apparatus was interfaced to a VIC 20 computer. Through software, the time for filling or emptying could be readily changed and the system programmed to stop at any cycle or run continuously.

Before using any samples in cycling tests, they were evacuated in the vessel to less than 10^{-4} mmHg and heated to 200°C by wrapping the sample vessel with Glas-Col heating tape. This tape was removed before the commencement of a cycling test.

The apparatus was checked out initially using Calgon BPL and Anderson AX-21 (previously Amoco GX-31) carbons. The BPL carbon was 12 to 40 mesh granules, while the AX-21 was larger, 6 to 12 mesh granules.

2.2/ Preparation of Saran Carbon Samples

Saran is the trade name of the Dow Chemical Company for a wide range of copolymers, all of which have vinylidene chloride as their principal

constituent. The homopolymer, 100% polyvinylidene chloride(PVDC), which in this report will be called Saran A, a designation used by Dow, is not made commercially. A small quantity of this was given to the authors by Dow Chemical. They also supplied Saran 415, a copolymer with 15% vinyl chloride, which has a melting point of about 165°C. Collectively, copolymers with vinyl chloride are known as Saran B resins.

These polymers are supplied as fine powders which can be ball-milled to produce "flours," if desired. They can be put in molds or dies and compressed at room temperature to a specific shape. Figure 3 plots the density of the resultant material versus the pressure used in compression. Pressures above 103.4 MPa (15 000 psi) show little increase in density. At pressures above 68.91 MPa (10 000 psi) the material is compact enough to be drilled or machined without fragmentation.

On heating, PVDC decomposes with loss of hydrogen chloride. If this loss of hydrogen chloride is continued to completion, a carbon, referred to as Saran carbon, results. The mechanism of this decomposition has been investigated by several workers [8,13,14]. The morphology of the carbon, however, is dependent on the method of preparation. If heating is carried out fairly rapidly, melting takes place first, followed by evolution of hydrogen chloride, which causes the melt to foam. The resulting carbon is irregularly shaped and has a large macropore volume as well as a micropore structure.

Macropore volume is undesirable in methane adsorption since it is, in effect, void volume. Carefully controlled heating over a long period, where the polymer degrades considerably below its melting point, can prevent melting by producing a highly cross-linked char, which on further slow heating to 700°C under nitrogen or vacuum, results in a carbon which is almost completely microporous and which has retained the shape of the original polymer but has shrunk linearly by about 25%. By using this latter technique, specifically shaped pieces of carbon can be made so that they can be packed together in a vessel and minimize dead space within the vessel.

It was thought that the simplest way to fill the sample vessel with minimum dead space was to prepare "cookie"- or "puck"-shaped pieces of Saran

carbon with a diameter equal to the inside diameter of the sample vessel and fill the vessel by stacking the disks of carbon on top of each other.

Two steel dies were made of appropriate diameter. A minimum pressure of 103.4 MPa (15 000 psi) was used to form the disks. One die was used for pressing disks of 100% polymer. The other, of lesser diameter, was used to press disks from a ball-milled mixture of 80% polymer and 20% by weight of the previously prepared Saran carbon. Since the polymer loses 75% of its weight as hydrogen chloride, after pyrolysis these disks would have 50% by weight original carbon and 50% freshly prepared carbon. The incorporation of the carbon was to try and prevent deformation and/or blistering during pyrolysis by providing a passage for the hydrogen chloride to escape.

Differential scanning calorimetry (DSC) was carried out on the polymer. This showed two temperature zones where great exothermicity occurs: one at 185 to 210°C and an even greater one from 460 to 530°C. Great care must be taken in these temperature regions to ensure the reaction rate is slow; otherwise, the heat of the reaction will cause a further increase in temperature. It is suspected, but not confirmed, that blistering and foaming are likely to occur in the lower temperature region, whereas cracking seems to be the result of too rapid a temperature rise in the higher temperature region.

It is easier to pyrolyse Saran A, possibly because it does not melt or because it is 100% PVDC, and produce blemish-free disks than from Saran B. Disks prepared from 100% Saran B were frequently blistered or distorted after heating to 250°C. Starting with a carbon/polymer mixture, either Saran A or Saran B, however, reduces the likelihood of blistering, etc. Many different rates of heating were tried, most resulting in failure to produce a "perfect" disk. A slow heating program was finally devised and generally produced blemish-free disks. No doubt, with further experimentation, this slow procedure can be improved upon. No difference was noted in the carbon produced, whether the pyrolysis was carried out in vacuum or under nitrogen. One disadvantage in using the carbon/polymer mixture was that the resulting carbon disk had a lower bulk density (the volume of the disk measured geometrically) than those

produced from 100% polymer, approximately 1.00 compared to 1.10 g/mL.

The disks used in the cycle tests were prepared from an 80% Saran B copolymer/20% Saran carbon mixture.

3/ CYCLING TESTS

Commercial purity grade (99.0%) methane was used in all the tests. No accumulation of impurities or loss in adsorption capacity was observed in any of the tests carried out. Natural gas, however, has been shown by Golovoy [2] to cause a reduction in adsorptive capacity of 9LXC carbon on repeated cycling, by accumulated adsorption of butanes and higher hydrocarbons.

A fill time of 15 min was selected. From the plot in Figure 4 for the Saran carbon, it can be seen that 93% of the equilibrium value at 25°C is reached in this time. The equilibrium value was taken as the value reached after a fill time of 2.5 h. This percentage is similar for the other carbons.

During filling, a peak temperature of 75°C was reached when using the AX-21; BPL and Saran carbon were about 10°C lower. This was measured by a bare thermocouple buried in the carbon. When a metal thermocouple well tube was used the recorded peak temperatures were some 10°C lower.

The drop in temperature on emptying was dependent on the rate at which the vessel was emptied. If it was emptied in 5 min or less, temperatures as low as -10°C were measured. An emptying time of 105 min was used. At this rate the temperature in the vessel never dropped more than a few degrees below ambient and had reached ambient again before filling on the next cycle. Figure 5 shows the time/temperature plots for a slow and a rapid emptying.

Table 4 shows the densities of the carbons used in the cycle tests. From these, and using a graphite density of 2.2 g/mL, the volume percent of vessel utilization can be calculated. Only the micropore volume is useful for methane adsorption. Figure 6 gives the linear relationship when this micropore volume is plotted against the amount of methane in the storage vessel at 2.067 MPa (300 psia), the pressure used in the cycle tests. This micropore volume will be the volume of all pores of less than 3 nm diameter, since this is the limiting diameter for mercury intrusion at 413.5 MPa (60 000 psi).

The results from the cycle tests are given in Table 5. Because the apparent or packing density of Saran carbon is considerably higher than BPL or AX-21 (Table 4), the amount of the methane stored in the Saran carbon-filled vessel is 90% greater than the AX-21-filled and 79% greater than the BPL-filled vessel at 2.067 MPa (300 psia). At 3.445 MPa (500 psia), 92 g of methane per litre were stored. This is 85% of the methane in a 13.78 MPa (2000 psi) cylinder of compressed gas (108 g/L).

These experimental results have been compared to predicted values based on the results obtained on small samples in a previous report [15]. They are shown in Table 6. All the experimental results give values a little lower than calculated. This is to be expected since rapid filling resulted in a substantial temperature rise and did not allow sufficient time to reach equilibrium, while the calculated results are based on a 25°C equilibrium isotherm.

The amount of methane delivered from storage vessels employing carbon adsorbents has been reported by Remick [5] to be from 84 to 94% of the total stored at 3.445 MPa (500 psig). The present results for AX-21 would also fall into this category.

Saran carbon adsorbs 3% by weight methane at 25°C and 1 atm pressure. At 2.067 MPa (300 psia), it adsorbs a little more than 9%; thus, one-third of the adsorbed methane will not be released when the pressure drops to 1 atm. At 2.067 MPa (300 psia) only 70% of the total methane in the vessel was delivered (57.3 g/L); this rose to 74% at 3.445 MPa (500 psia) (68.0 g/L) (see ratio in Table 5). In spite of these low percentages, the amount of methane delivered is still higher than from any adsorbent reported to date.

This could be improved if the sample could be warmed.

From experimental isotherms with small samples on a Cahn microbalance, at 50°C Saran carbon adsorbs 2% by weight methane and at 70°C, 1.5% at 1 atm.

If the storage vessel were to be warmed to 50°C, a further 9.0 or 66.3 g methane per litre total from 2.067 MPa (300 psia) would be delivered (81%), while at 70°C this value increases to 71.3 g methane per litre from 2.067 MPa (300 psia) or 87% of the total stored in the vessel.

These results are summarized in Table 7. The goal of 108 g methane per litre delivered, equal to the amount from a 13.78 MPa (2000 psi) compressed cylinder, has not been reached for pressures less than 3.445 MPa (500 psia), but it is closer than ever before.

4/ ACTIVATION OF SARAN CARBON

4.1/ Steam Activation

The carbon used in this study was prepared from Saran A by pressing it into 1.9-cm-diameter (0.75-in.-diameter) pellets approximately 6.35 mm (0.25 in.) thick, which were slowly pyrolysed to 700°C under nitrogen. They were degassed at 200°C under vacuum ($<10^{-5}$ mmHg) and weighed under vacuum. To activate, the samples were placed in a quartz tube and the tube placed in a tube furnace. Nitrogen was passed into a steam generator, and the nitrogen steam mixture passed over the carbon heated to 800°C at 50 to 100 mL/min. About an 8% loss occurred after 3 h. This was determined by degassing at 200°C and weighing under vacuum. Weight loss was approximately linear with time of activation.

Samples with various weight losses up to 45% were prepared.

To ensure that activation had been carried out homogeneously throughout these carbon samples and was not just an outer bulk surface effect, a similar activation process was conducted on small Saran carbon pellets of 0.7 to 1.2 mm diameter. They are identified in the tables as SCP samples. The results obtained suggest that, indeed, homogeneous activation of the larger samples was achieved.

The densities from high pressure mercury intrusion porosimetry are given in Table 8 for the different percent weight loss carbons, often referred to as burn-off. The linear relationship between density and burn-off can be seen in Figure 7. Also included in the table is the apparent or packing density of the sample in the volumetric apparatus used to measure the methane adsorption isotherm. Calculated from these densities is the volume percent utilization of the sample storage vessel. Figures 8 and 9 plot the mercury intrusion per gram of sample with pressure for different percent burn-off. The large increase in macropore volume for the higher percent burn-off samples is evident.

Nitrogen isotherms at 77 K were carried out on all the samples. From this isotherm it has been customary to calculate a surface area using the BET equation [11]:

$$P/V(P_s - P) = 1/cV_m + (P/P_s) \times (c - 1)/cV_m$$

where P = pressure
V = volume adsorbed
P_s = saturation pressure
V_m = volume of monolayer
c = constant

The very high BET areas obtained with carbons have been criticized as being unrealistic because the assumptions of the BET equation are not being met with such highly microporous solids [16]. Surface areas can also be calculated by applying, to the nitrogen isotherm, either the Langmuir equation,

$$P/(x/m) = P/V_m + 1/bV_m$$

where (x/m) = mass fraction of adsorbed gas
b = constant

or the Dubinin equation,

$$\text{Log}\ (x) = \text{Log}\ (W_o\rho) - D\ [\text{Log}\ (P_s/P)]^2$$

where W_o = micropore volume
ρ = liquid density
D = constant
x = mass of adsorbed gas

Lamond and Marsh [9], for carbon-dioxide-activated Saran carbons, found the Dubinin equation to give generally lower values of surface areas than the BET equation. Surface area values for the present samples are higher using the Dubinin equation. These values are listed in Table 9, along with values calculated using the 25°C methane isotherm. Regardless of what equation is used, it can be seen that the surface area per gram of sample increases fairly linearly with increasing percent burn-off. Plots of surface area versus percent burn-off are shown in Figures 10 and 11. The ratio of the 25°C methane surface area to the 77 K nitrogen surface area, whether calculated from Dubinin or Langmuir, remains reasonably constant with increasing percent burn-off.

Little or no relationship between total or cumulative pore volume per gram of adsorbent and the amount of methane adsorbed per gram has been found for commercially available carbons [3,5], while a relationship between BET surface area (77 K nitrogen isotherm) and methane adsorption at ambient temperatures was found. This is to be expected.

Total or cumulative pore volumes, including pores of up to 20 nm diameter, can be calculated by the Barrett, Joyner, and Halenda method [17] from a desorption isotherm. Since methane adsorption at 25°C takes place in micropores (diameters less than 2 nm), the micropore volume should be a better parameter for assessing potential methane adsorption by microporous materials, not the sum of the micropore and the macropore volume.

If an oversimplified model of cylindrical pores is considered and an arbitrary pore volume of 0.5 mL/g is chosen, then pores of 20 nm diameter would have a surface area of only 100 m^2/g, while pores of 2 nm diameter would have an area of 1000 m^2/g. Thus, large-diameter pores (macropores) contribute little to surface area but can contribute greatly to total pore volume, while micropores have large surface areas per gram for a similar volume.

The consequence of this is that there is a close relationship between surface area and/or micropore volume and methane adsorption for highly microporous materials, whereas there will be no relationship between total or cumulative pore volume and methane adsorption.

Carbons with large cumulative pore volumes often have large macropores and, subsequently, low bulk densities. Even though they may have considerable micropore volume, from a practical standpoint, where unit volume, and not unit mass, of adsorbent must be considered, they will not be as useful as adsorbents with similar micropore volume but with little or no macropore volume.

Table 10 lists the macropore volume obtained form mercury intrusion for the activated Saran carbons. This is graphed in Figure 12, where the great increase for samples with more than 30% burn-off can clearly be seen.

The micropore volume per gram, calculated using the Langmuir and Dubinin equations on the 77 K nitrogen isotherm, are also in Table 10. Both equations give similar values, which are linear with percent burn-off (Figure 13). In a previous publication [18], the authors showed that micropore volumes from a methane isotherm at 77 K were similar to those measured from a nitrogen isotherm at 77 K for several different carbons, suggesting that the nitrogen molecule and the methane molecule can enter similarly sized pores.

Neglecting void volume, from a unit volume consideration, because the density of the carbon is decreasing as burn-off increases, the micropore volume per millilitre also increases. This would be linear if the macropore volume remained constant. The large increase in macropore volume above 30% burn-off negates any increase in micropore volume per millilitre of total volume. This is illustrated graphically in Figure 14. The dip at 5% is also attributable to the increase in macropore volume.

Thus, if micropore volume per unit volume is the critical factor in methane adsorption at ambient temperatures, then an increase in methane adsorption per unit volume is to be expected for samples with up to 30% burn-off. Above this value, macropore formation is taking place more rapidly than micropore formation, and so from a volume consideration, no increase in methane adsorption would be predicted.

4.1.1/ Methane Adsorption

Methane adsorption isotherms at 25°C were measured at pressures up to 10.34 MPa (1500 psia) on all the steam-activated Saran carbons in the high pressure volumetric apparatus described previously [15]. They show a steady increase in methane adsorbed per gram carbon with increasing percent burn-off (Figures 15 and 16). The difference in methane adsorbed is more apparent at higher pressures. This is illustrated in Figure 17, where the amount of methane adsorbed per gram at several pressures is shown versus the percent burn-off. The relationship is reasonably linear.

Initially this seems encouraging, a gain of 30% in methane adsorbed at 2.067 MPa (300 psia) and an even greater increase at higher pressures in going from a 0 to 45% burn-off carbon.

At the same time, however, there has been a considerable decrease in the density of these carbon adsorbents, and so from a volume of adsorbent consideration there is, in fact, little or no increase in the methane stored. Figure 18 shows the amount of methane stored per unit volume of adsorbent (void space, since it is variable depending on how well the sample vessel was packed, has been neglected). The most significant feature of these plots is how similar they are in distribution to those in Figure 14, where micropore volume per unit volume of adsorbent is plotted.

This gives an indication of how important the role of the micropore is in the adsorption of methane at ambient temperatures. It also emphasizes the effect that increasing macropore volume has on methane adsorption. Any gains made by increasing micropore volume are nullified whenever the macropore volume becomes larger. This is, in fact, what was predicted from the measured micropore and macropore volumes for the various burn-off carbons.

Figure 19 is a plot showing the density of the adsorbed methane in the micropore versus percent burn-off. Both the Dubinin and Langmuir micropore volumes have been used, and the close similarity in values is obvious.

Dubinin plots have been made for the 25°C methane isotherms; these are shown in Figure 20. From the intercept, the saturation value for methane adsorption at this temperature can be evaluated, and using the Dubinin micropore volume from the 77 K nitrogren isotherm, a saturation density, gram methane per millilitre of micropore, can be found. The saturation densities for methane at 25°C for the different burn-off carbons, calculated from the Dubinin and Langmuir equations, are plotted in Figure 21. The values are remarkably constant, about 25% lower than the density of methane at its normal boiling point (0.41 g/mL at 111 K) but nearly twice the critical density (0.16 g/mL). The degree or efficiency of filling of the micropore at various pressures for each carbon can then be calculated

by dividing the methane density in the micropore with the saturation density. A list of values is given in Table 11, and they are plotted for some pressures in Figure 22.

At these pressures, the degree of saturation, which can be looked on as the extent to which the pore can be filled, remains reasonably constant up to 20% burn-off. At higher percent burn-off, the pores are not filled as much by the methane, suggesting that the micropore diameter plays an important role in the adsorption process. As burn-off progresses, the micropore volume increases, probably by enlarging the size of existing pores rather than creating new pores. With increased pore volume, some of the methane molecules in the pore will be further away from the influence of the wall or surface of the pore and will not pack together as closely as when they are on the surface, and consequently, the efficiency to which the pore is filled will be less. From Figure 22 it can be seen that this is particularly true at lower pressures, but at higher pressures the change is less apparent. At 2.067 MPa (300 psia) the pore is filled to about 70% of saturation; this increases with pressure, so at 6.891 MPa (1000 psia) the value is over 80%. However, it is evident that there is no gain in methane density with increasing burn-off.

A similar analysis can be carried out using the Langmuir equation. Plots of this for the 25°C methane isotherm of the various burn-off carbons are given in Figure 23. From the reciprocal of the slope, the Langmuir saturation density for methane can be found. Values are listed in Table 12 and are plotted in Figure 21. These values parallel the Dubinin values but are about 10% lower.

Also included in Table 12 are the methane densities in the micropore at several pressures for the different burn-off carbons. These, like the Dubinin values, have been used to calculate the degree of saturation achieved in the micropore at various pressures. Figure 24 shows the extent of micropore filling for the different burn-off carbons at different pressures. As with the Dubinin plot, Figure 22, it is evident that the efficiency of filling the micropore diminishes as percent burn-off increases.

4.1.2/ Conclusion on Steam Activation

Activation by steam of Saran carbon at 800°C results in a loss of carbon. This is expressed in a percent weight loss (burn-off). Both bulk and mercury (413.5 MPa or 60 000 psi) densities decrease with increasing burn-off. The difference of the reciprocal of these densities gives a measure of the macropore volume. This increases a little for low percent burn-offs, but above 30%, burn-off increases unacceptably if any gain in adsorption per unit volume is to be achieved.

The micropore volume as measured from either density, Dubinin or Langmuir, increases steadily with percent burn-off from a weight consideration. There is also a corresponding increase in surface area per gram of carbon. When the volume of carbon is considered, however, there is no significant increase in micropore volume over the percent burn-off range investigated. Since methane adsorption occurs in the micropores, no appreciable gain in methane storage should be expected, and very little was observed at the lower pressures. Some improvement was observed at 6.891 MPa (1000 psi).

Had there been no macropore volume increase, then there would have been an increase per unit volume in the micropore volume as the burn-off increased. This would result in more methane being adsorbed per unit volume.

4.2/ Heat Treatment Activation

In a recent publication [12], it was claimed that Saran carbon prepared by rapidly heating (2°C/min) Saran polymer to 900°C under nitrogen and then to temperatures up to 1300°C under helium showed enhanced adsorption. The result was a more microporous carbon for heat treatment up to 1100°C, while at 1300°C the carbon structure shrunk and some micropore volume was lost.

If a simple procedure such as this could produce a carbon with increased adsorption to methane, then this would be easy to do and could improve the performance of our present 700°C Saran carbons.

To that end, Saran carbon samples, prepared by slow pyrolysis of the polymer to 700°C under nitrogen or vacuum, were heated up to 1000 and 1100°C under nitrogen, the final temperature being maintained for 4 h.

The resulting samples were then examined by mercury intrusion (Figure 25) and by 77 K nitrogen isotherm to determine their various densities, macropore and micropore volume, and BET surface area. The values obtained are given in Table 13, along with the values for the normally produced 700°C carbon. Within experimental limits, there was no change in these properties with heat treatment.

Methane isotherms at 25°C are shown in Figure 26, along with the isotherm of the 700°C carbon. The isotherms are coincident for pressures to 4.135 MPa (600 psia), with little deviation above this pressure.

It must, therefore, be concluded that heat treatment of Saran carbons to 1100°C will not enhance their adsorptive capacity to methane at 25°C.

5/ REFERENCES

[1] Barton, S.S., Dacey, J.R., Evans, M.J.B., Holland, J.A., and Quinn, D.F., "Report on OJT & CRP Project 33353," Ministry of Transportation and Communications, Government of Ontario, March 1984.

[2] Golovoy, A. and Blais, E.J., "Alternate Fuels for Spark-Ignition Engines," Report SP-559, Society of Automotive Engineers, R 47, 1983.

[3] Innes, R.A., Lutinski, F.E., Occelli, M.L., and Kennedy, J.V., US Department of Energy Report CE 50071, July 1984.

[4] Otto, K., "Alternative Energy Sources IV," Vol 6, R 241, Ann Arbor Science, 1982.

[5] Remick, R.J., Elkins, R.H., Camara, E.H., and Bulicz, T., US Department of Energy and NASA Report 0327-1, June 1984.

[6] Everett, D.H., Pure and Applied Chem. 31:579, 1972.

[7] Dubinin, M.M., Progress in Surface and Membrane Science, edited by D.A. Cadenhead et al, Vol 9, p. 1, Academic Press, 1975.

[8] Kipling, J.J. and Wilson, R.B., Trans Faraday Soc. 56:557, 1960.

[9] Lamond, T.G. and Marsh, H., Carbon 1:923, 1964.

[10] Culver, R.V. and Heath, N., Trans Faraday Soc. 51:1569, 1955.

[11] Braunauer, S., Emmett, P.H., and Teller, E., J. Amer. Chem. Soc. 60:309, 1938.

[12] Fernandez-Morales, I. et al, Carbon 22:301, 1984.

[13] Dacey, J.R. and Barradas, R.G., Can. J. Chem. 41:180, 1963.

[14] Winslow, F.H. et al, Proc. 1st and 2nd Carbon Conf., U. of Buffalo Press, p. 93, 1956.

[15] Barton, S.S., Dacey, J.J., Evans, M.J.B., and Quinn, D.F., "Report on OJT and CPR Project 33258," Ministry of Transportation and Communications, Government of Ontario, December 1982.

[16] Halsey, G.D., "The Gas-Solid Interface," Vol. I & II, edited by E.A. Flood and Marcel Dekker, 1967.

[17] Barrett, E.P., Joyner, L.G., and Halenda, P.P., J. Amer. Chem. Soc. 73:373, 1951.

[18] Barton, S.S., Dacey, J.R., and Quinn, D.F., in "Fundamentals of Adsorption," edited by A.L. Myers and G. Belfort, Amer. Inst. of Chem. Eng., p. 65, 1983.

Table 1/ IUPAC* Classification of Pores by Size

Macropores	Widths > 50 nm
Mesopores	Widths > 2 nm and < 50 nm
Micropores	Widths < 2 nm

Mercury intrusion at 413.5 MPa (60 000 psi) is considered to fill all pores > 3 nm.

*International Union of Pure and Applied Chemistry

Table 2/ Density Definitions

$$\text{Apparent or Packing} = \frac{\text{wt of carbon in adsorption vessel}}{\text{vol of vessel}}$$

$$\text{Bulk} = \frac{\text{wt of carbon}}{\text{vol of displaced Hg at 1 atm}}$$

$$\text{Bulk} = \frac{\text{wt of carbon}}{\text{measured volume of carbon}}$$

$$\text{Mercury, 413.5 MPa (60 000 psi)} = \frac{\text{wt of carbon}}{\text{vol of displaced Hg at 413.5 MPa (60 000 psi)}}$$

Table 3/ Volume Utilization
(Calculated from Data from Reference 1)

Empty Vessel
methane at 2.412 MPa (350 psia)

16.1 g/L

Any Carbon Adsorbent

C carbon
M macropore
V void
μ micropore

Saran Carbon (0.70) g/mL
methane at 2.412 MPa (350 psia)

4.5 g/L gas
66.0 g/L adsorbed
70.5 g/L total

Amoco GX-32 (0.30 g/mL)
methane at 2.412 MPa (350 psia)

7.7 g/L gas
42.0 g/L adsorbed
49.7 g/L total

Table 4/ Density Volume Relationships

Carbon	BPL	AX-21	Saran B (cracked samples)	Saran B
Apparent Density				
g/mL	0.51	0.30	0.84	0.93
lb/ft^3	(31.8)	(18.8)	(52.5)	(58.1)
Bulk Density				
g/mL	0.80	0.45	0.90	1.00
lb/ft^3	(50.0)	(28.1)	(56.3)	(62.5)
Mercury Density				
g/mL	1.26	1.00	1.20	1.20
lb/ft^3	(78.8)	(62.5)	(75.0)	(75.0)
Volume Percent				
Carbon	23.2	13.6	38.2	42.3
Micropore	17.3	16.4	31.7	35.2
Macropore	23.3	36.7	23.3	15.5
Void	36.2	33.3	6.8	7.0

Table 5/ Cycling Test Results

Carbon	BPL	AX-21	Saran B (cracked samples)	Saran B	
# of Cycles	12	20	100	20	20
Fill Time (min)	15	15	15	15	15
Empty Time (min)	105	105	105	105	105
Pressure MPa	2.1	2.1	2.1	2.1	3.4
psi	300	300	300	300	500
Methane in Vessel					
g/L	45.6	43.0	74.8	81.5	92.2
scf/ft^3	68.8	65.5	112.9	123.0	139.1
Methane Output					
g/L	32.4	38.1	49.7	57.3	68.0
scf/ft^3	49.0	57.4	75.0	86.4	102.6
Compressed Methane					
g/L	13.8	13.8	13.8	13.8	23.6
scf/ft^3	20.9	20.9	20.9	20.9	35.6
Advantage in Vessel	3.3	3.1	5.4	5.9	3.9
Advantage Delivered	2.5	2.9	3.8	4.3	3.0
Ratio Delivered in Vessel	0.71	0.88	0.66	0.70	0.74

Table 6/ Predicted Methane Storage

Carbon	BPL	AX-21	Saran B (cracked samples)	Saran
Density (g/mL)				
Apparent	0.51	0.30	0.84	0.93
Bulk	0.80	0.45	0.90	1.00
Mercury	1.26	1.00	1.20	1.20
Volume Percent				
Carbon	23.2	13.6	38.2	42.3
Micropore	17.3	16.4	31.7	35.2
Macropore	23.3	36.7	23.3	15.5
Void	36.2	33.3	6.8	7.0
Methane adsorbed in carbon at 25°C, 2.067 MPa (300 psia), g/g	0.074	0.127	0.091	0.091
Carbon g/L	510	300	840	930
Methane adsorbed g/L	37.7	38.1	76.4	84.6
Methane gas g/L	8.2	9.7	4.2	3.1
Total methane (gas + ads.) g/L	46.0	47.8	80.6	87.7
Experimental value (gas + ads.) g/L	45.6	43.0	74.8	81.5
Void + macropore volume, with methane gas at 13.8 g/L and 2.067 MPa (300 psia), L/L	0.595	0.700	0.300	0.225

Table 7/ Summary of Cycle Tests

Carbon		BPL	AX-21	Saran B
Density				
g/L		510	300	930
lb/ft^3		31.8	18.8	58.1
Methane				
Stored in vessel at	g/L	45.6	43.0	81.5
2.067 MPa (300 psia)	scf/ft^3	68.8	65.5	123.0
delivered from 2.067 MPa (300 psia)				
at 25°C	g/L	32.4	38.1	57.3
	scf/ft^3	49.0	57.4	86.4
at 50°C	g/L			66.3*
	scf/ft^3			100.0
at 70°C	g/L			71.3*
	scf/ft^3			107.6
Stored in vessel at 3.445 MPa	g/L			92.2
(500 psia)	scf/ft^3			139.1
delivered from 3.445 MPa (500 psia)				
at 25°C	g/L			68.0
	scf/ft^3			102.6
at 50°C	g/L			77.0*
	scf/ft^3			116.2
at 70°C	g/L			82.0*
	scf/ft^3			123.7
108 g/L or 163 scf/ft^3 of methane are stored in in an empty vessel at 13.78 MPa (2000 psia)				

*Estimated

Table 8/ Steam-Activated Saran Carbons -- Mercury Porosimetry

Percent Burn-Off Carbon (Standard or SCP)	0.0 STD	5.7 STD	11.8 STD	20.7 STD	28.0 STD	35.8 SCP	37.3 STD	45.0 SCP	45.4 STD
Density (g/mL)									
Apparent	0.70	0.63	0.59	0.58	0.55	0.44	0.51	0.41	0.48
Bulk	1.10	1.05	1.01	0.94	0.88	0.72	0.77	0.70	0.73
Mercury, 413.5 MPa (60 000 psi)	1.20	1.20	1.16	1.10	1.04	0.97	0.98	0.95	0.92
Volume Percent									
Carbon	31.8	28.6	26.8	26.4	25.0	20.0	23.2	18.6	21.8
Micropore	26.5	23.9	22.4	26.3	27.9	25.4	28.9	24.5	30.4
Macropore	5.3	7.5	9.3	9.0	9.6	15.8	14.2	15.4	13.6
Void	36.4	40.0	41.6	38.3	37.5	38.9	33.8	41.4	34.2

Table 9/ Steam-Activated Saran Carbons -- Surface Area (m^2/g)

Percent Burn-Off Carbon (Standard or SCP)	0.0 STD	5.7 STD	11.8 STD	20.7 STD	28.0 STD	35.8 SCP	37.3 STD	45.0 SCP	45.4 STD
77 K Nitrogen Isotherm									
BET	1000	1090	1140	1390	1620	1680	1720	1850	2000
Dubinin	1220	1220	1350	1580	1850	2000	1960	2225	2350
Langmuir	1200	1200	1325	1540	1775	1910	1860	2080	2165
25°C Methane Isotherm									
Dubinin	745	768	837	907	1013	1196	1111	1230	1268
Langmuir	652	656	750	827	892	998	987	1080	1105
Ratio of 25° Methane Area/77 K Nitrogen Area									
Dubinin	0.61	0.63	0.62	0.57	0.55	0.60	0.57	0.55	0.54
Langmuir	0.54	0.55	0.57	0.54	0.50	0.52	0.53	0.52	0.51

Table 10/ Steam-Activated Saran Carbons -- Micropore and Macropore Volumes

Percent Burn-Off Carbon (Standard or SCP)	0.0 STD	5.7 STD	11.8 STD	20.7 STD	28.0 STD	35.8 SCP	37.3 STD	45.0 SCP	45.4 STD
Micropore Volume									
Dubinin									
mL/g	0.43	0.43	0.48	0.56	0.65	0.71	0.69	0.79	0.80
mL/mL	0.45	0.43	0.45	0.48	0.51	0.51	0.44	0.55	0.46
Langmuir									
mL/g	0.42	0.42	0.47	0.54	0.63	0.67	0.66	0.73	0.76
mL/mL	0.44	0.42	0.45	0.47	0.50	0.48	0.44	0.51	0.46
Density									
mL/g	0.38	0.38	0.41	0.45	0.51	0.58	0.57	0.60	0.63
mL/mL	0.42	0.40	0.41	0.43	0.45	0.42	0.44	0.42	0.46
Macropore Volume									
Density									
mL/g	0.08	0.13	0.15	0.16	0.17	0.35	0.28	0.38	0.27
mL/mL	0.08	0.12	0.13	0.14	0.15	0.25	0.21	0.27	0.21

Table 11/ Steam-Activated Saran Carbons -- Methane Micropore Densities (Dubinin)

Percent Burn-Off Carbon (Standard or SCP)	0.0 STD	5.7 STD	11.8 STD	20.7 STD	28.0 STD	35.8 SCP	37.3 STD	45.0 SCP	45.4 STD
Dubinin Saturation Density (g methane/ mL micropore)	0.293	0.302	0.294	0.273	0.263	0.284	0.272	0.264	0.274
Methane Adsorbed (g/mL micropore) at 2.067 MPa (300 psia)	0.211	0.209	0.204	0.193	0.172	0.172	0.168	0.158	0.155
at 3.445 MPa (500 psia)	0.228	0.230	0.227	0.212	0.193	0.200	0.194	0.181	0.181
at 4.135 MPa (600 psia)	0.228	0.239	0.233	0.220	0.200	0.211	0.203	0.189	0.190
at 6.891 MPa (1000 psia)	0.237	0.258	0.250	0.234	0.223	0.232	0.223	0.211	0.214
Degree of Saturation at 2.067 MPa (300 psia)	0.722	0.693	0.690	0.706	0.655	0.605	0.618	0.651	0.578
at 3.445 MPa (500 psia)	0.778	0.762	0.767	0.778	0.737	0.704	0.714	0.688	0.676
at 4.135 MPa (600 psia)	0.790	0.792	0.789	0.804	0.760	0.742	0.745	0.731	0.710
at 6.891 MPa (1000 psia)	0.810	0.855	0.844	0.857	0.848	0.810	0.820	0.804	0.798

Table 12/ Steam-Activated Saran Carbons -- Methane Micropore Densities (Langmuir)

Percent Burn-Off Carbon (Standard or SCP)	0.0 STD	5.7 STD	11.8 STD	20.7 STD	28.0 STD	35.8 SCP	37.3 STD	45.0 SCP	45.4 STD
Langmuir Saturation Density (g methane/ mL micropore)	0.255	0.264	0.270	0.259	0.240	0.252	0.253	0.251	0.246
Methane Adsorbed (g/mL micropore) at 2.067 MPa (300 psia)	0.217	0.214	0.208	0.200	0.178	0.182	0.176	0.171	0.163
at 3.445 MPa (500 psia)	0.233	0.236	0.232	0.220	0.200	0.212	0.203	0.196	0.191
at 4.135 MPa (600 psia)	0.237	0.245	0.238	0.228	0.206	0.224	0.212	0.196	0.200
at 6.891 MPa (1000 psia)	0.243	0.264	0.255	0.242	0.230	0.246	0.233	0.220	0.225
Degree of Saturation at 2.067 MPa (300 psia)	0.850	0.812	0.772	0.772	0.741	0.722	0.695	0.682	0.663
at 3.445 MPa (500 psia)	0.914	0.893	0.859	0.851	0.833	0.841	0.802	0.721	0.776
at 4.135 MPa (600 psia)	0.930	0.928	0.882	0.878	0.861	0.888	0.838	0.814	0.813
at 6.891 MPa (1000 psia)	0.953	0.999	0.945	0.936	0.960	0.977	0.922	0.911	0.915

Table 13/ Heat Treatment -- Saran Carbons

Heat Treatment Temperature °C	700	1000	1100
Density (g/mL)			
Apparent	0.70	0.64	0.64
Bulk	1.10	1.03	1.06
Mercury, 413.5 MPa (60 000 psi)	1.20	1.13	1.17
Macropore Volume (mL/g)	0.08	0.09	0.09
77 K Nitrogen Isotherm			
BET Area (m^2/g)	1050	1020	1030
Dubinin Micropore Volume (mL/g)	0.45	0.43	0.43
25°C Methane Isotherm			
g methane ads. per g carbon			
2.067 MPa (300 psia)	0.093	0.093	0.090
3.445 MPa (500 psia)	0.102	0.100	0.100
4.135 MPa (600 psia)	0.103	0.102	0.102
6.891 MPa (1000 psia)	0.106	0.108	0.112

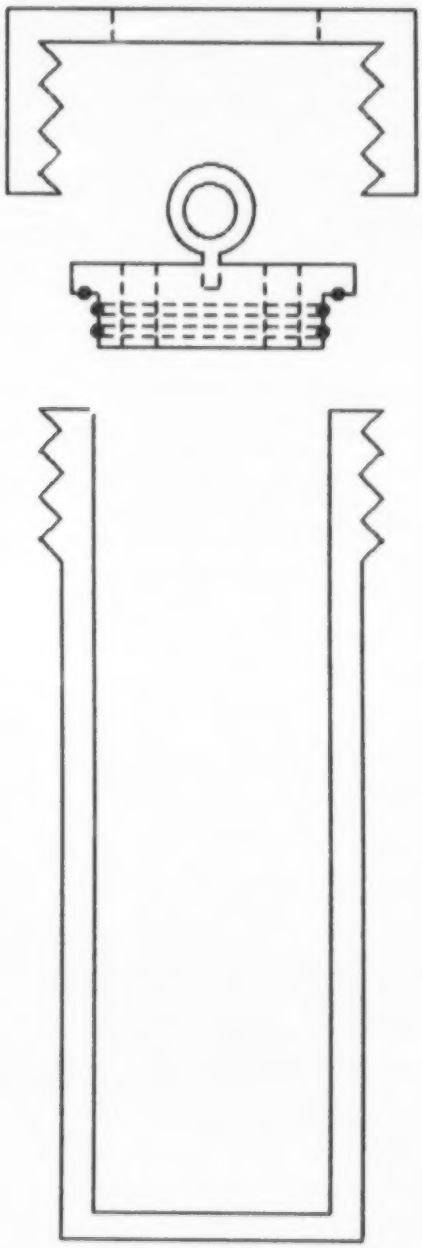

Figure 1/ One-Litre Sample Storage Vessel

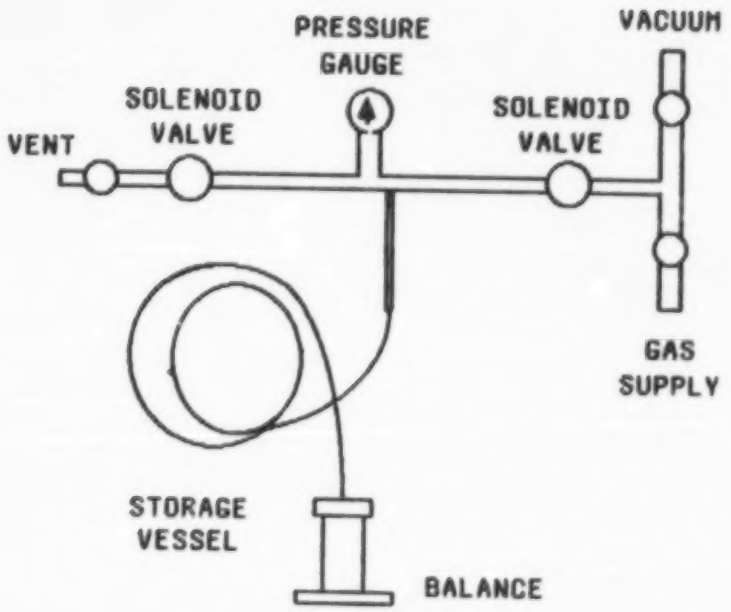

Controlled by a VIC 20 Computer

Figure 2/ Cycle Test Apparatus

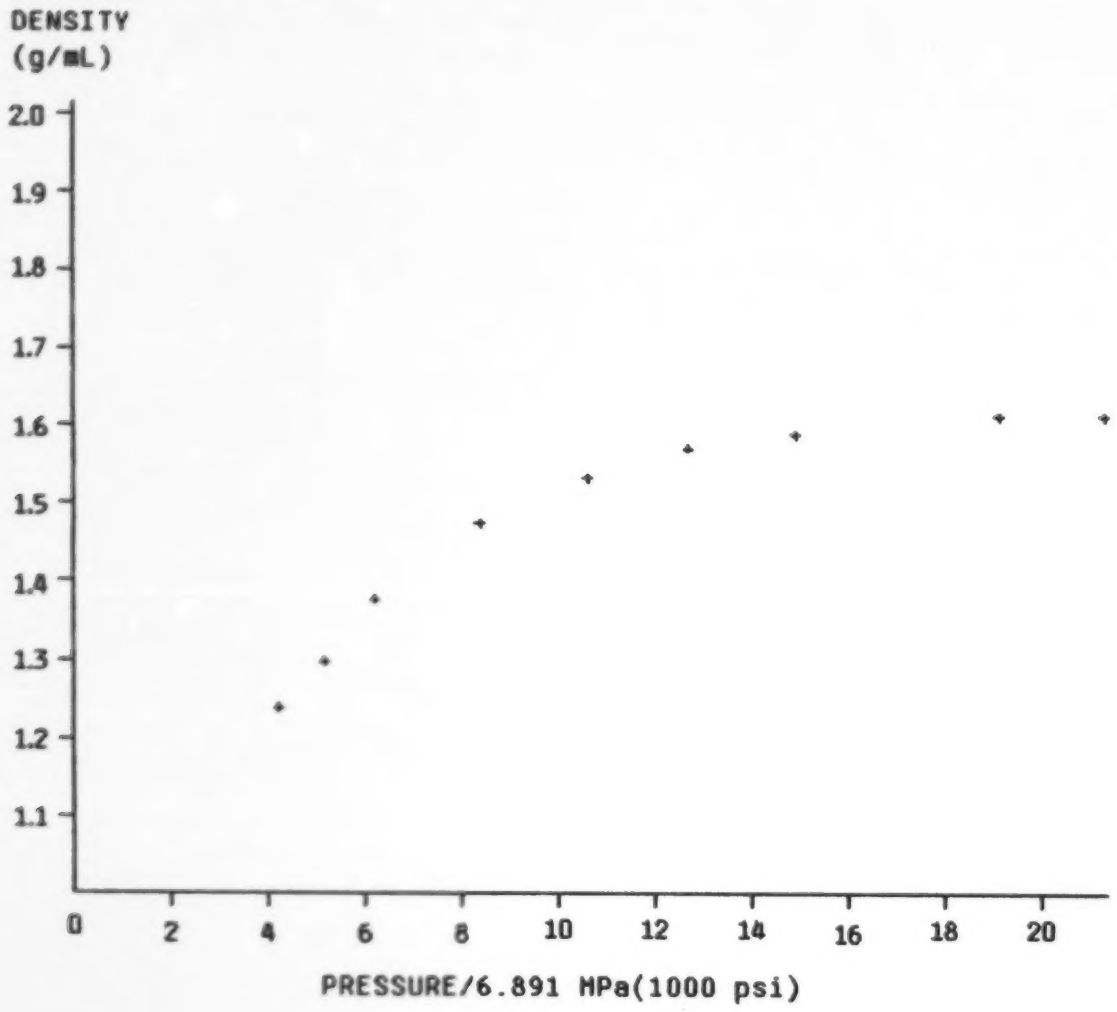

Figure 3/ Compression of Saran Polymer

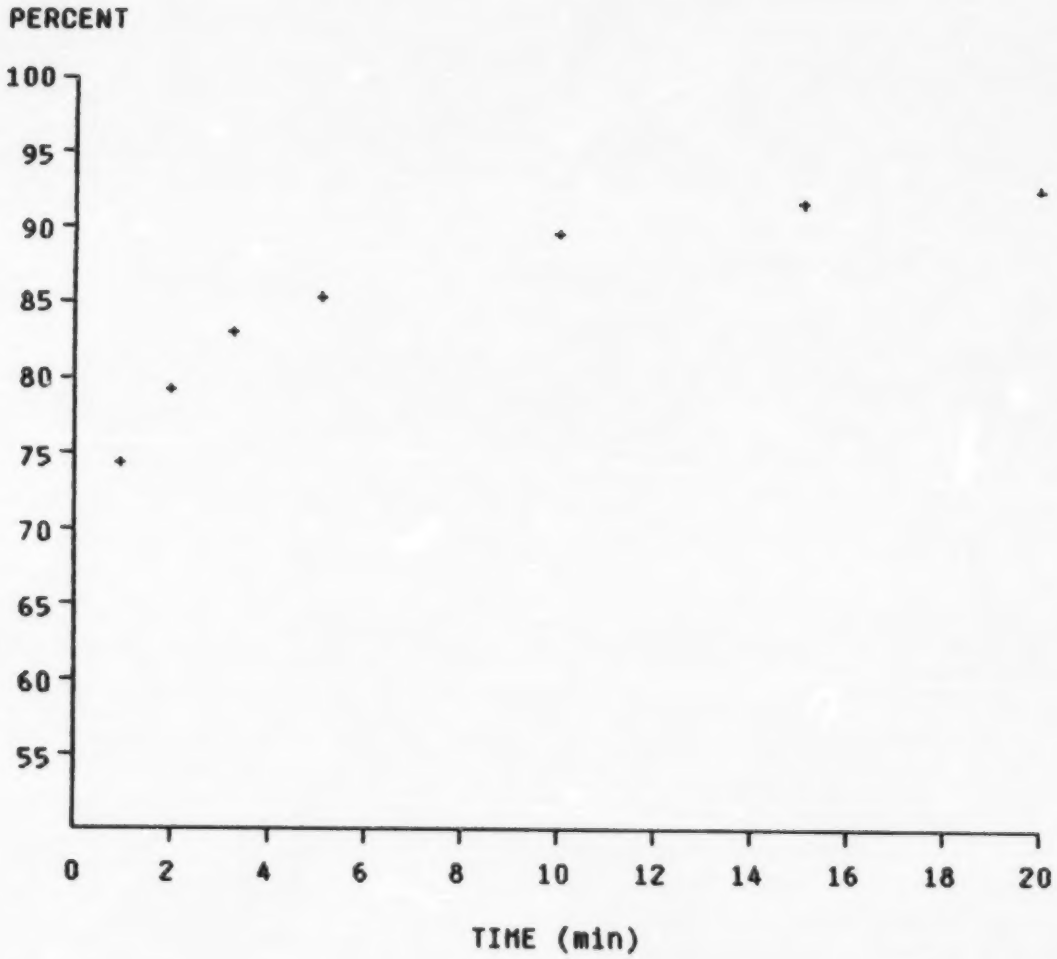

Figure 4/ Saran Carbon -- Percent of Methane Stored Relative to Saturation at 25°C and 2.067 MPa(300 psia) vs. Time

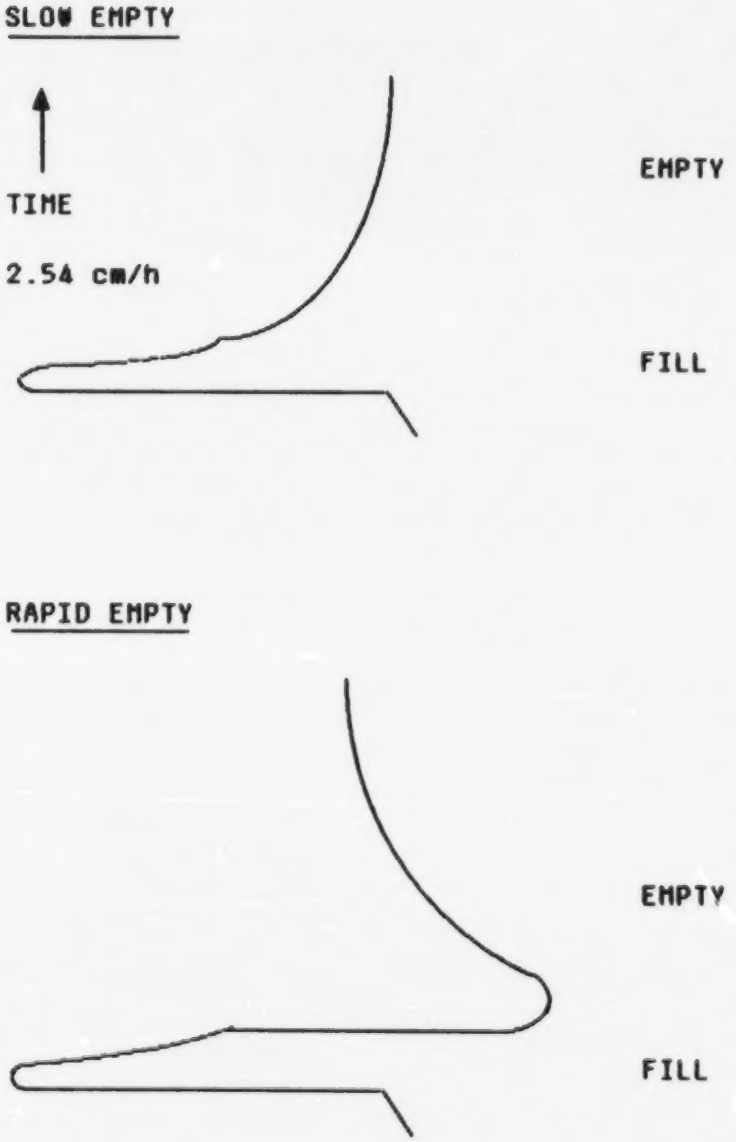

Figure 5/ Temperature Transitions During Filling and Emptying Saran Carbon with Methane

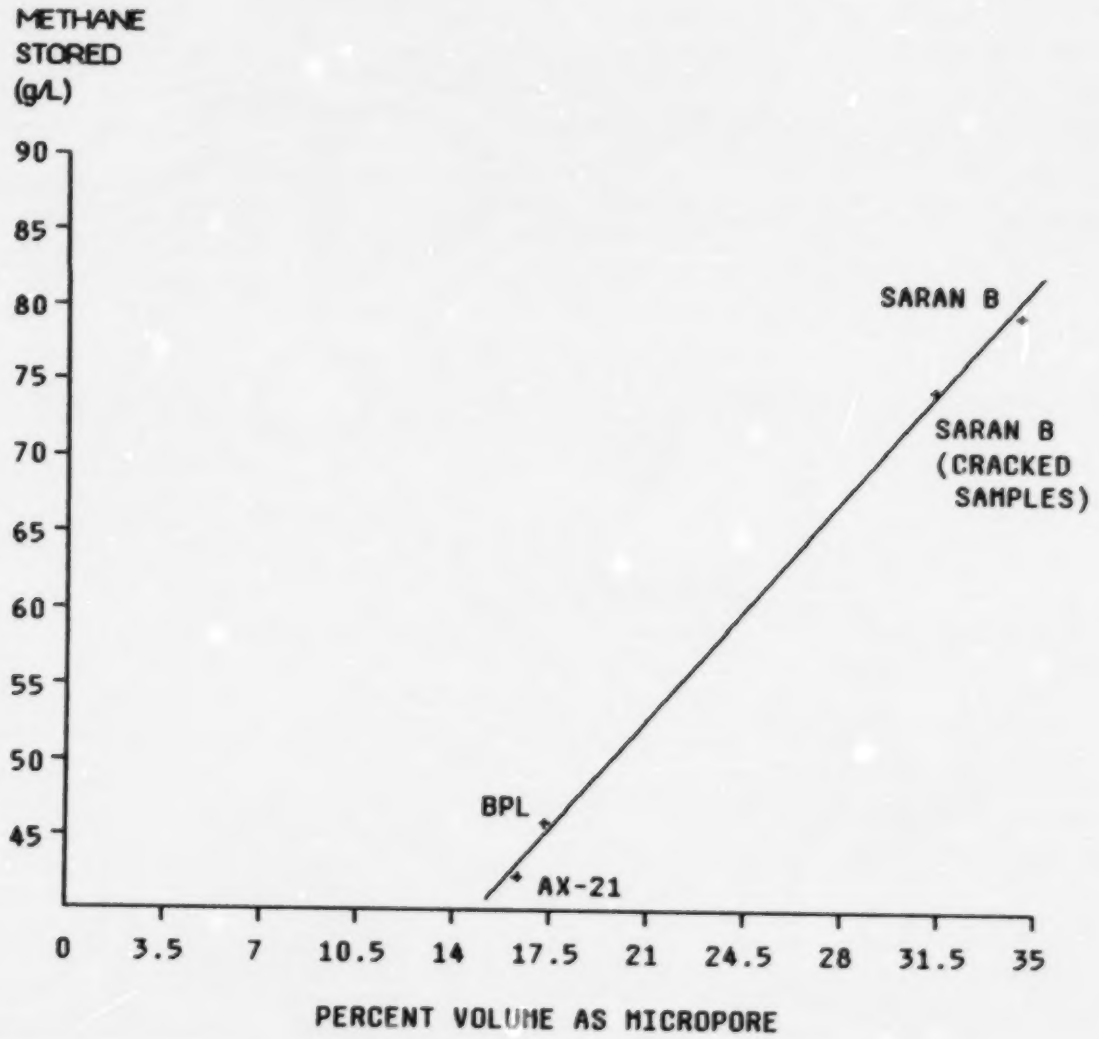

Figure 6/ Methane Stored at 2.067 MPa(300 psia) vs. Percent Volume as Micropore

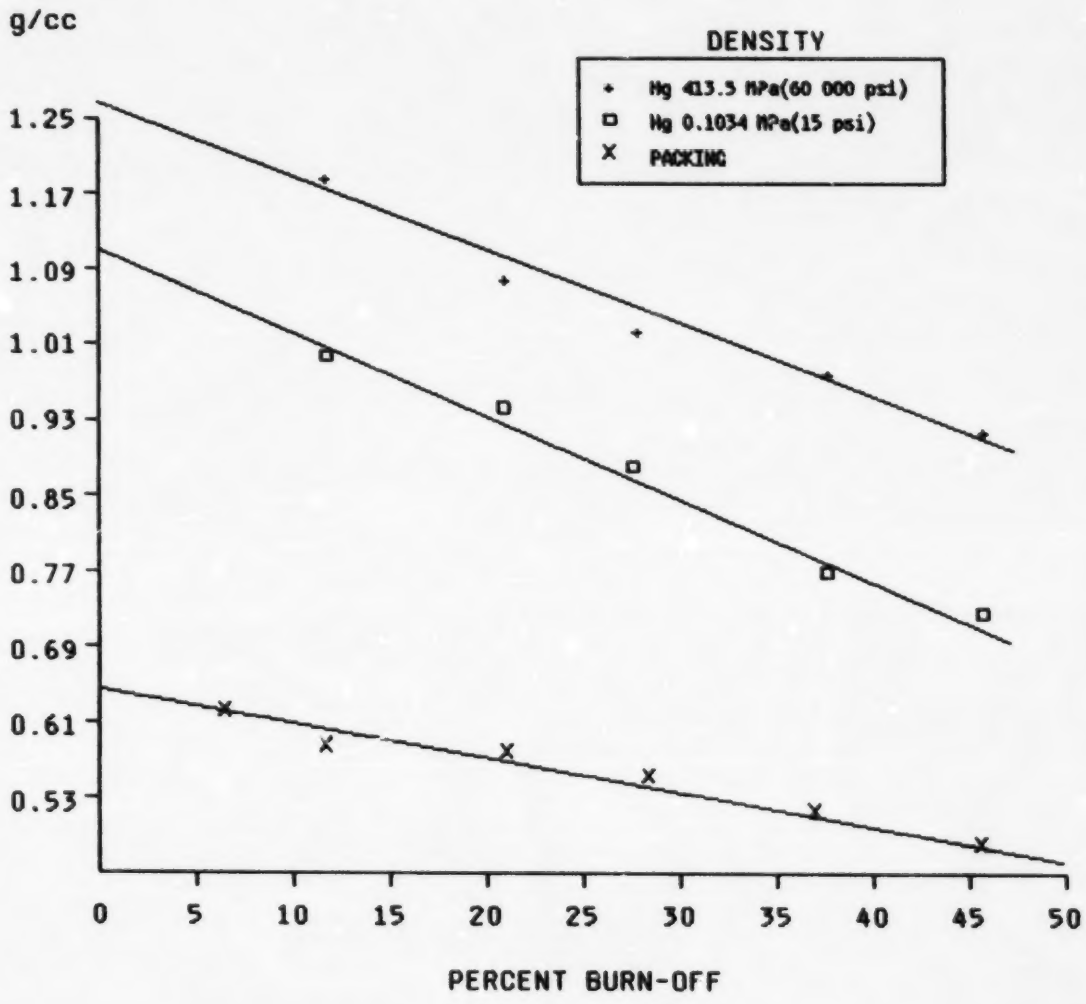

Figure 7/ Densities -- Steam-Activated Saran Carbon

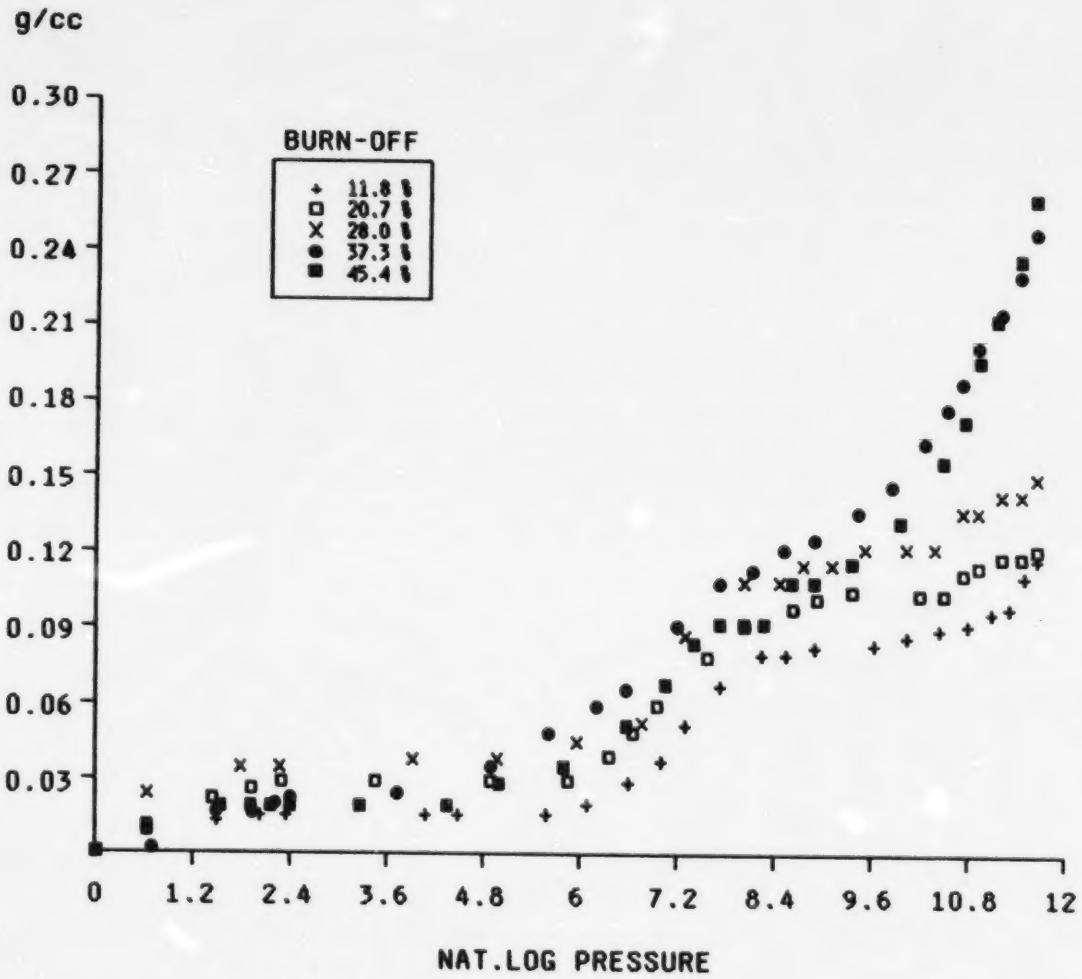

Figure 8/ Mercury Porosimetry -- Steam-Activated Saran Carbon

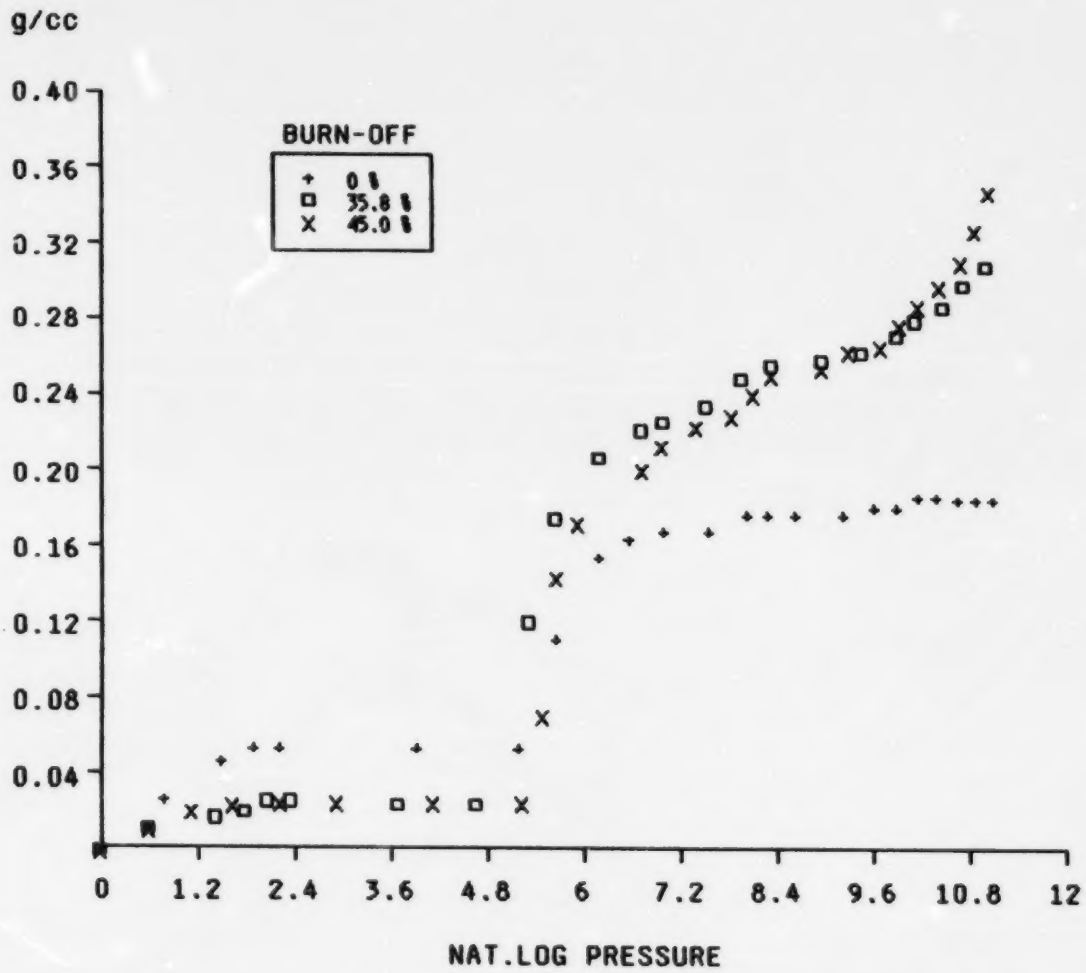

Figure 9/ Mercury Porosimetry -- Steam-Activated Saran Carbon Pellets

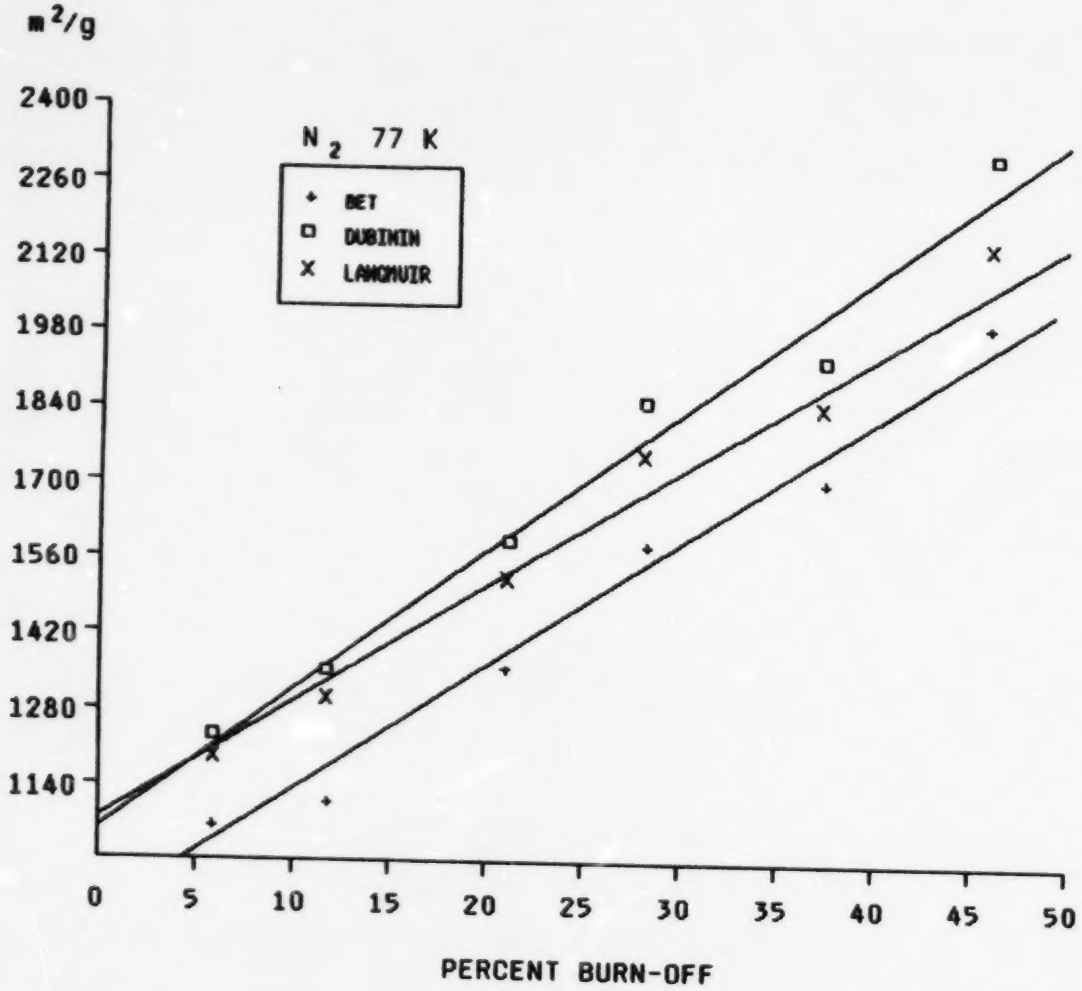

Figure 10/ Surface Areas -- Steam-Activated Saran Carbon

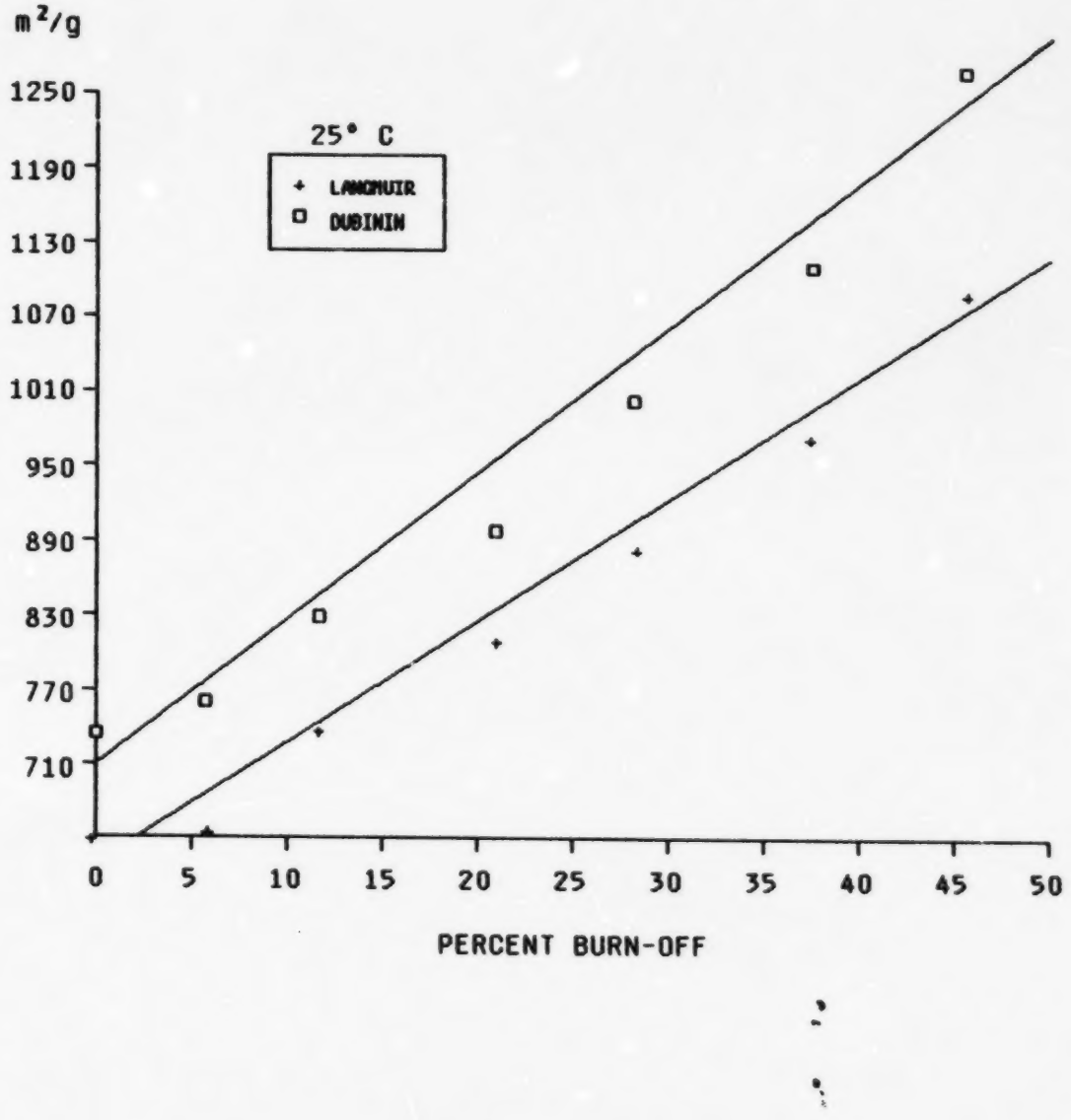

Figure 11/ Methane Surface Areas -- Steam-Activated Saran Carbon

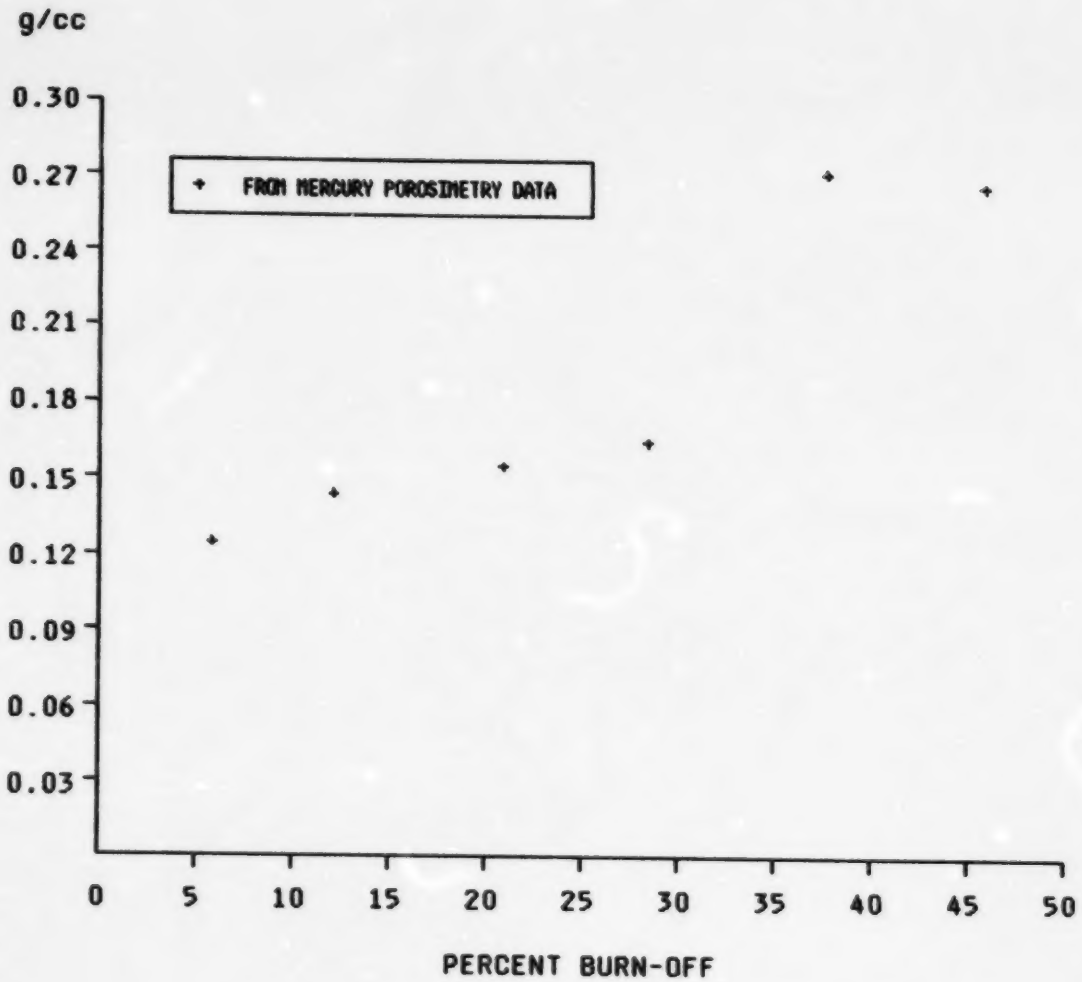

Figure 12/ Macropore Volume -- Steam-Activated Saran Carbon

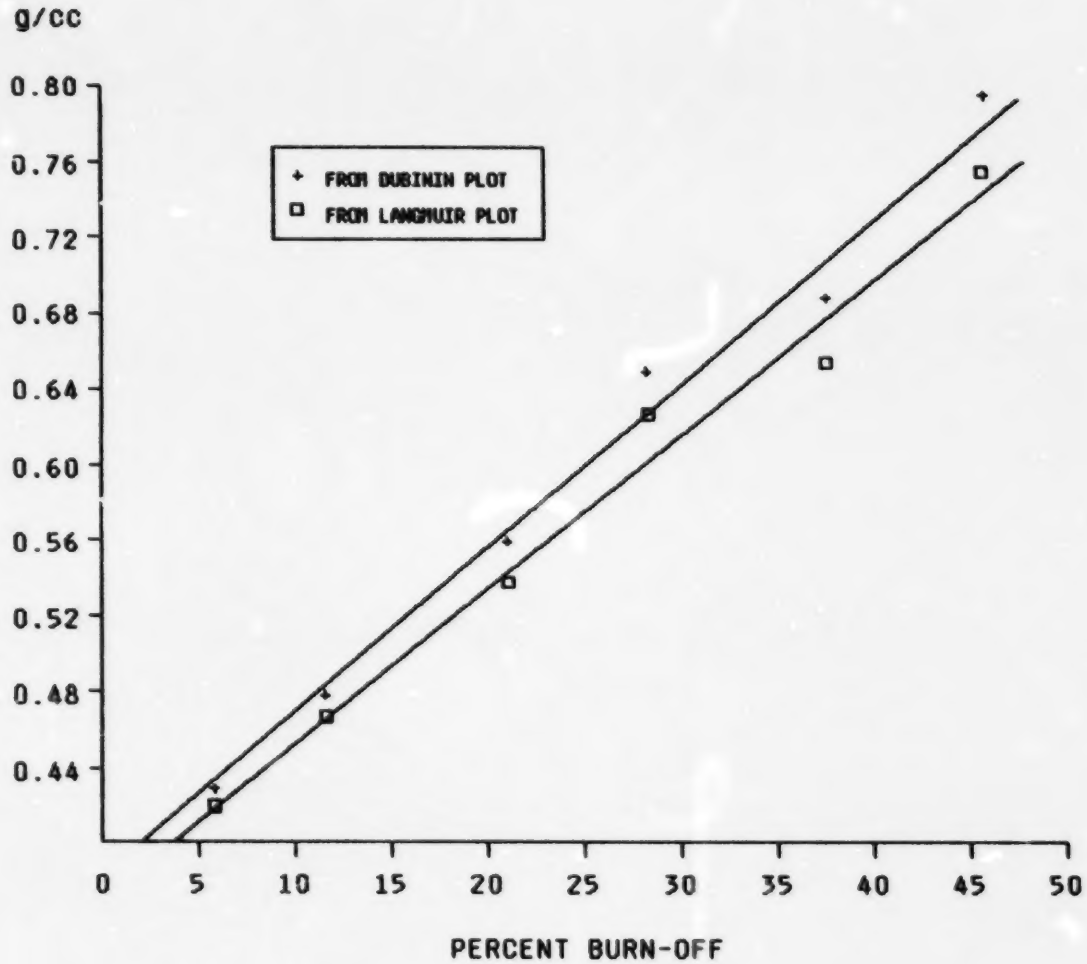

Figure 13/ Micropore Volume -- Steam-Activated Saran Carbon

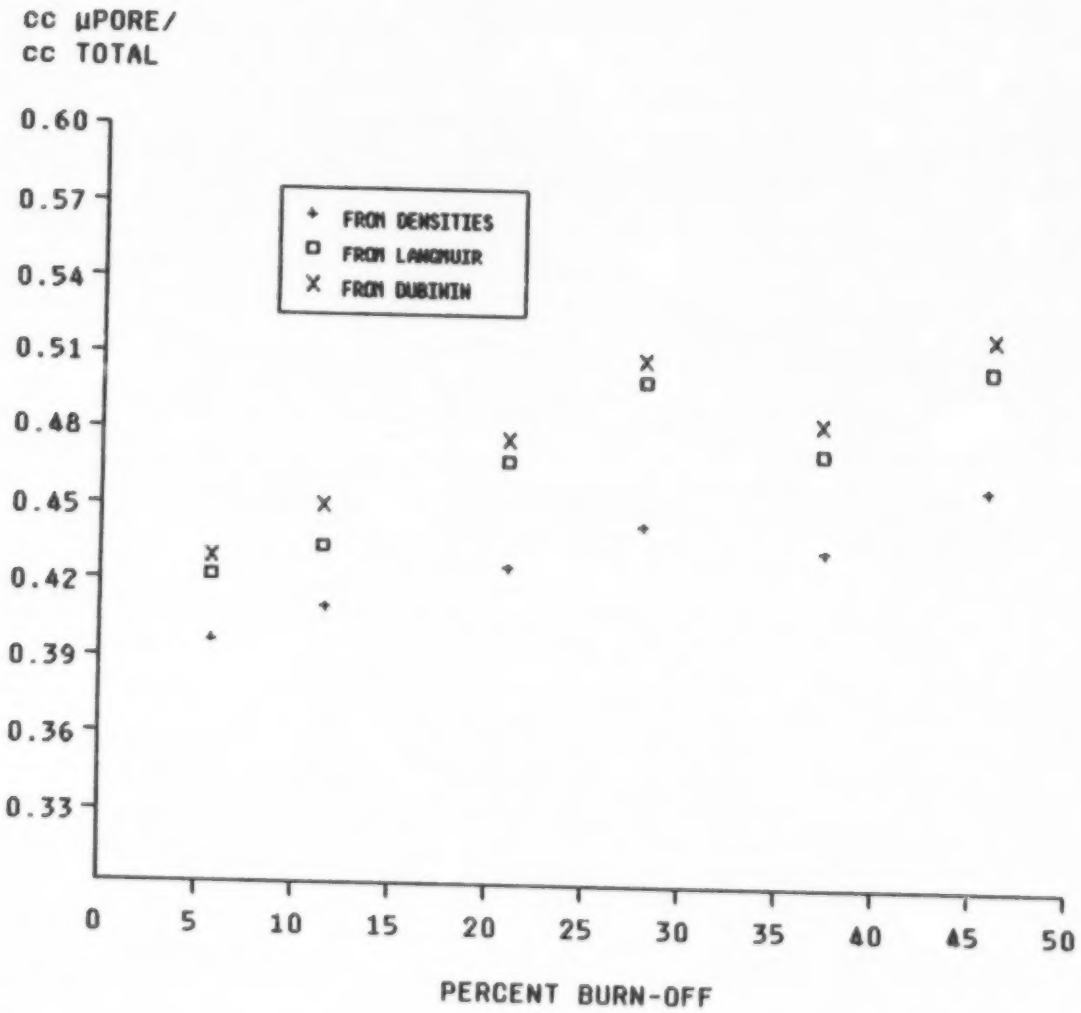

Figure 14/ Micropore Volume per Millilitre Total Volume -- Steam-Activated Saran Carbon

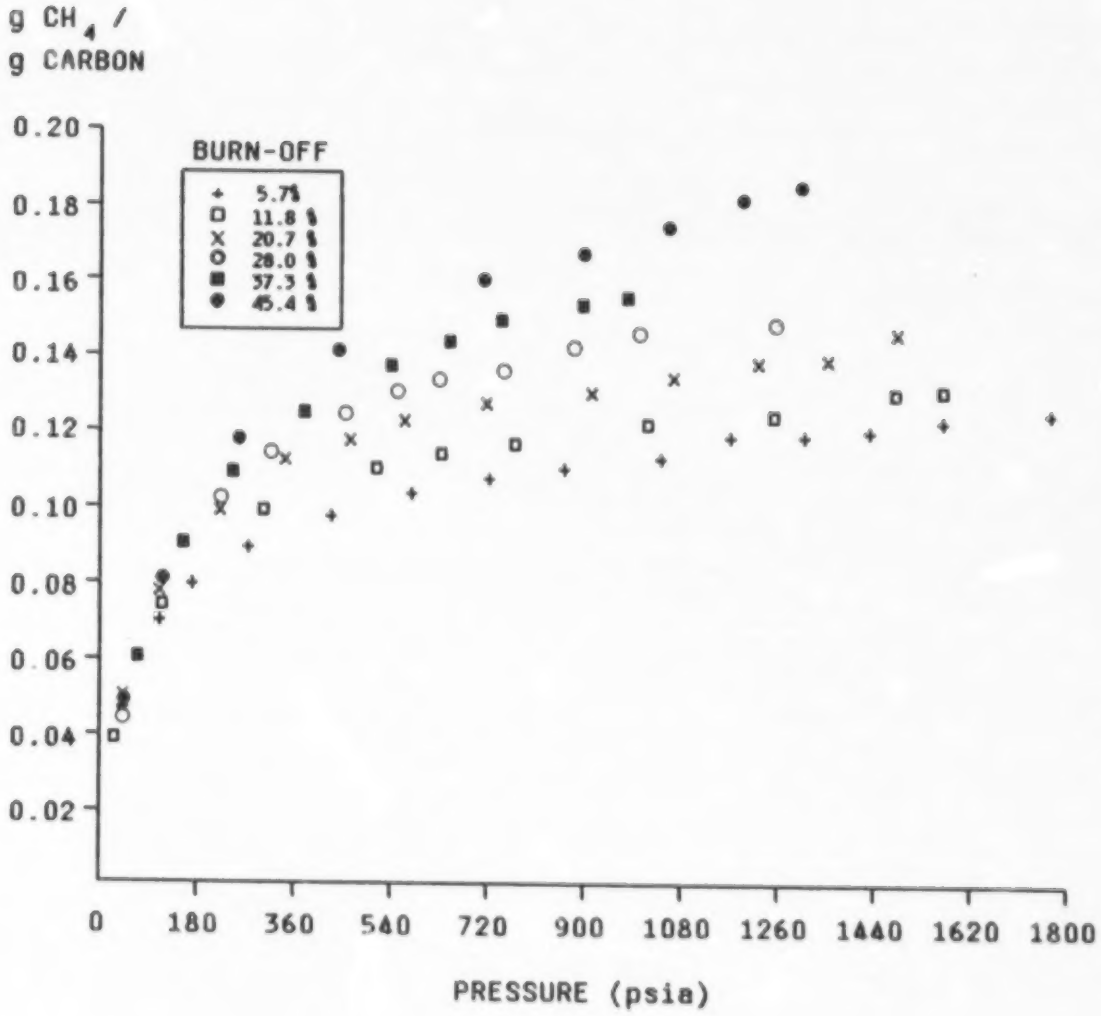

Figure 15/ Methane Adsorption Isotherms, 25° C -- Steam-Activated Saran Carbon

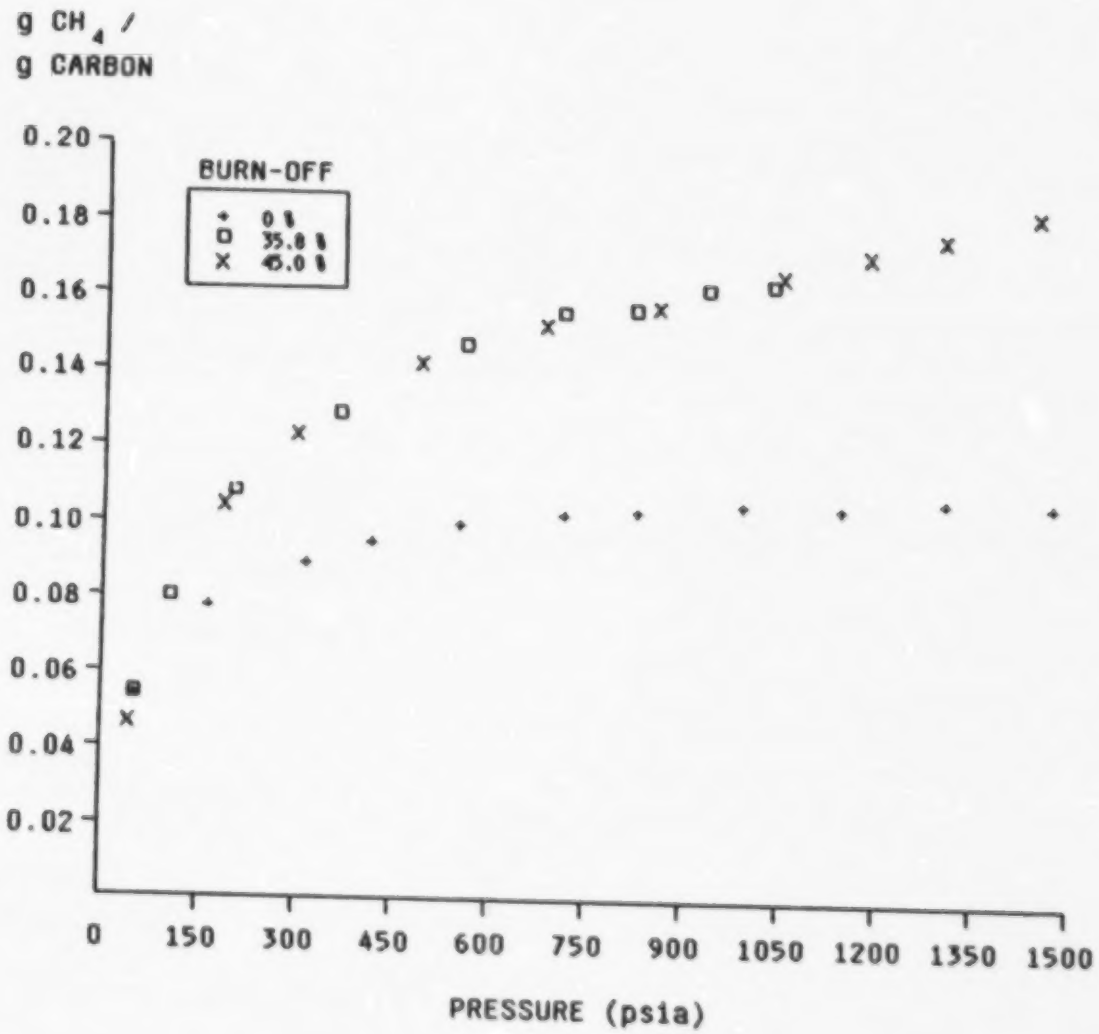

Figure 16/ Methane Adsorption -- Steam-Activated Saran Carbon Pellets

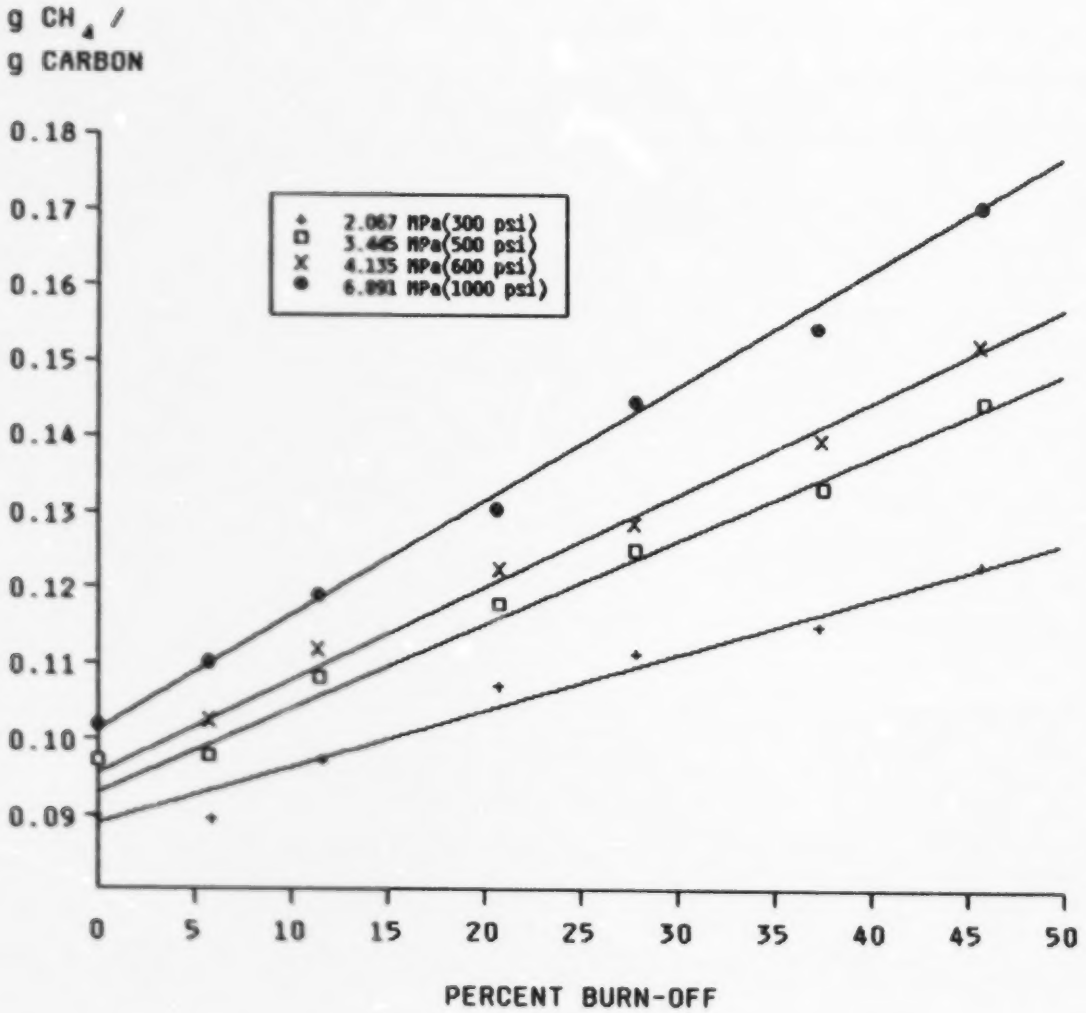

Figure 17/ Methane Adsorption, 25° C --
Steam-Activated Saran Carbon

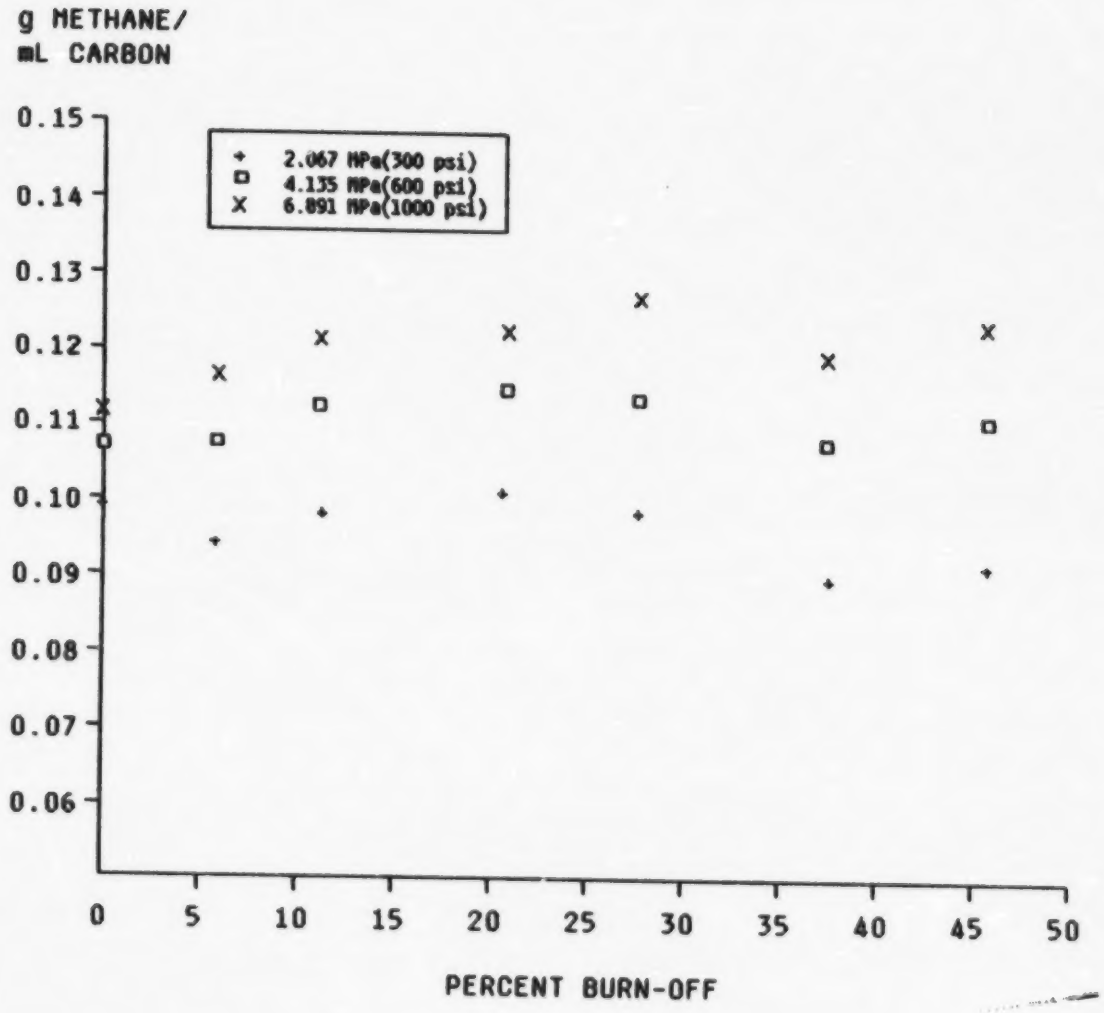

Figure 18/ Methane Adsorbed per Unit Volume Carbon -- Steam-Activated Saran Carbon

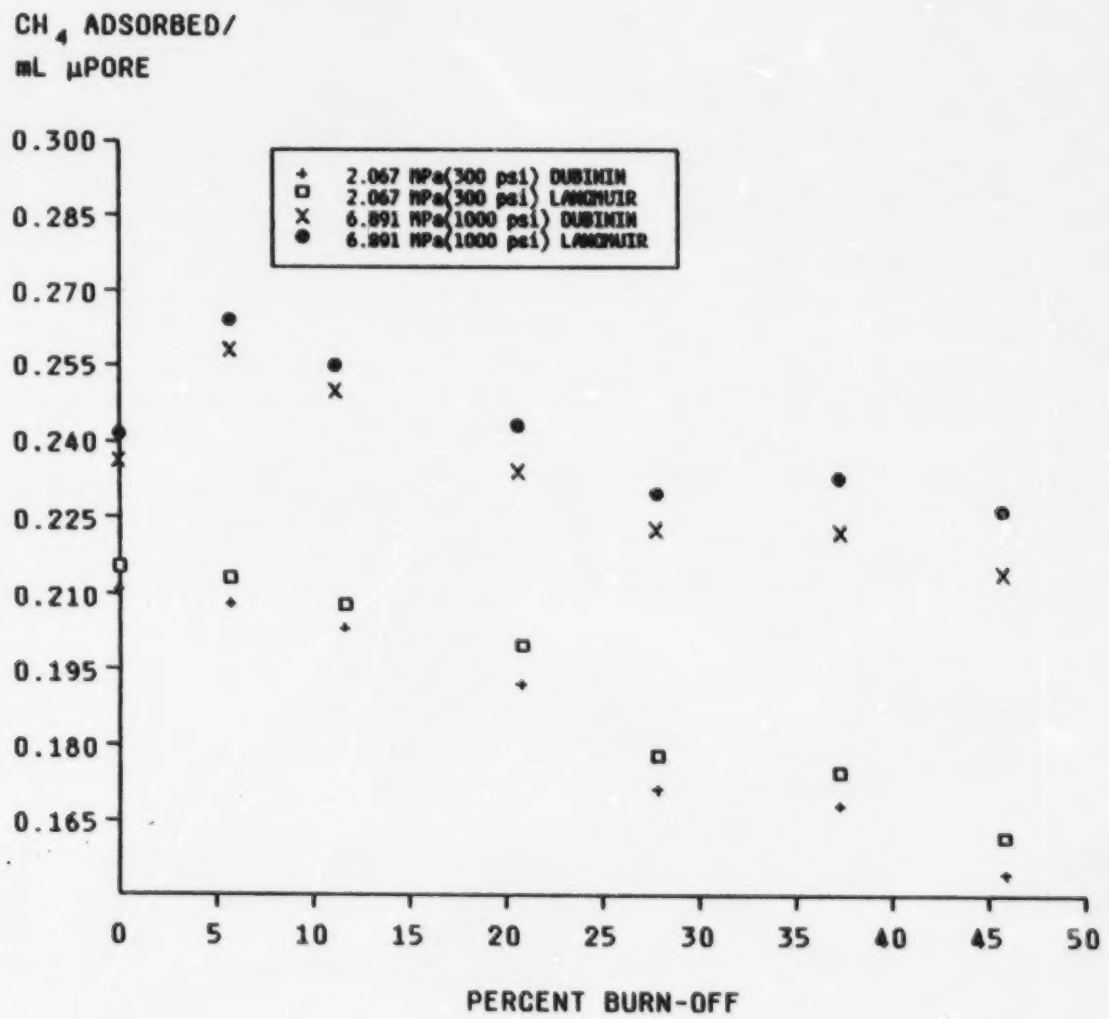

Figure 19/ Methane Adsorbed per Millitre of Micropore -- Steam-Activated Saran Carbon

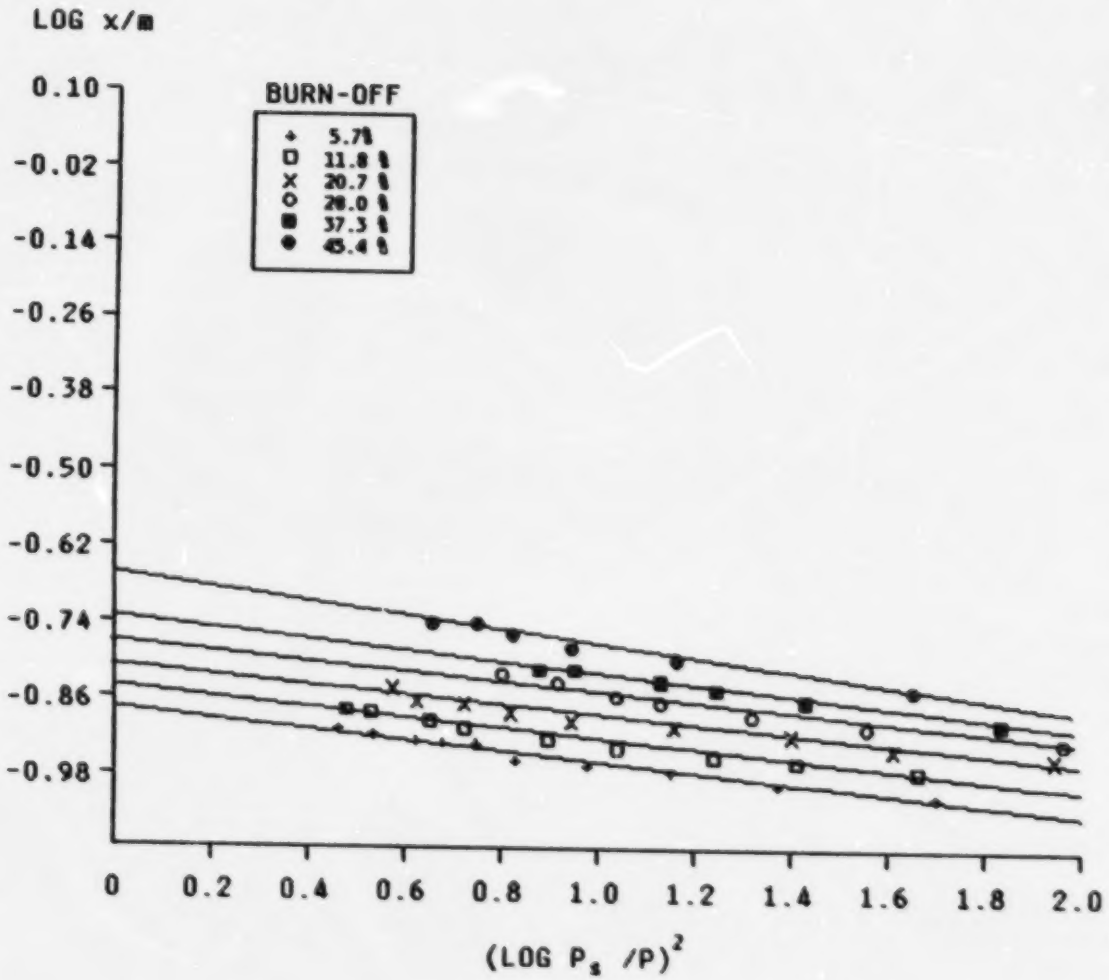

Figure 20/ Dubinin Plots -- Steam-Activated Saran Carbon

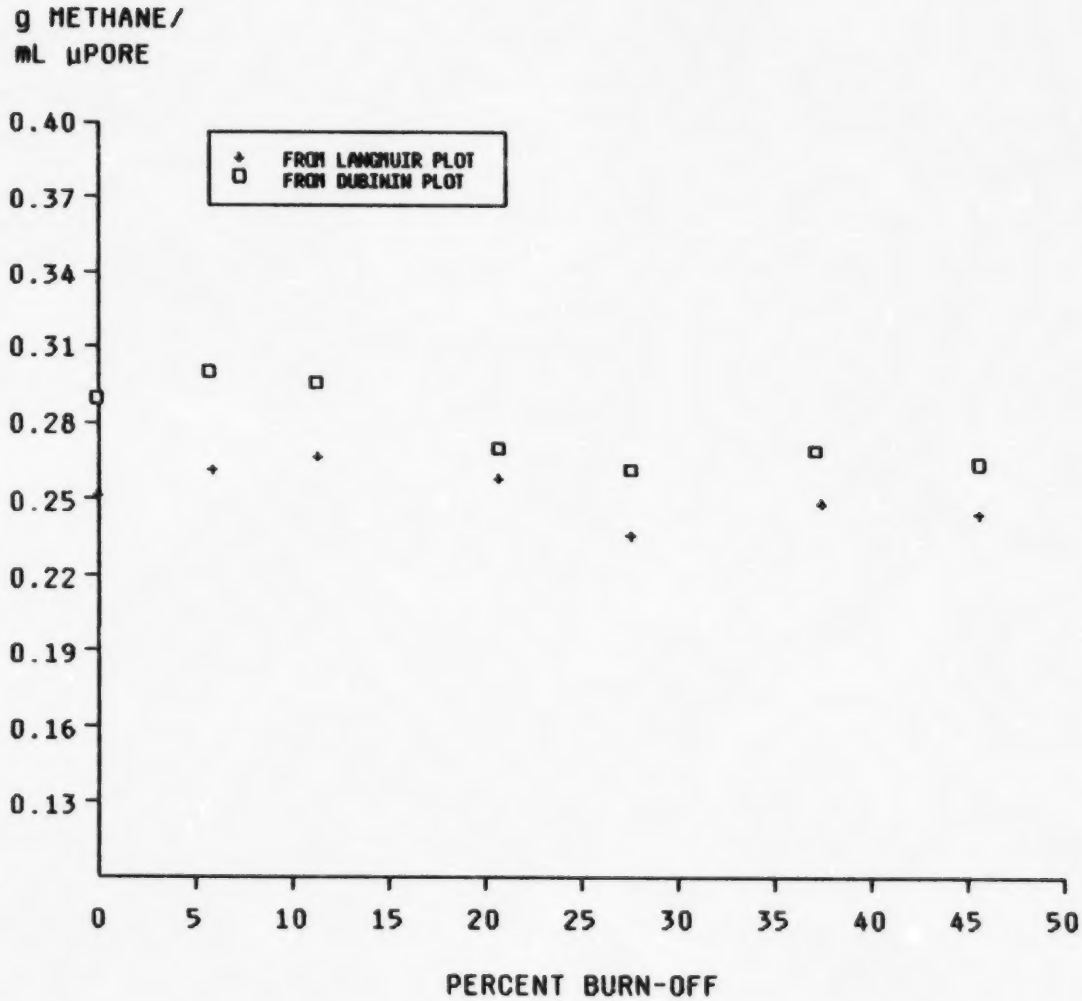

Figure 21/ Saturation Densities -- Adsorbed Methane, 25° C

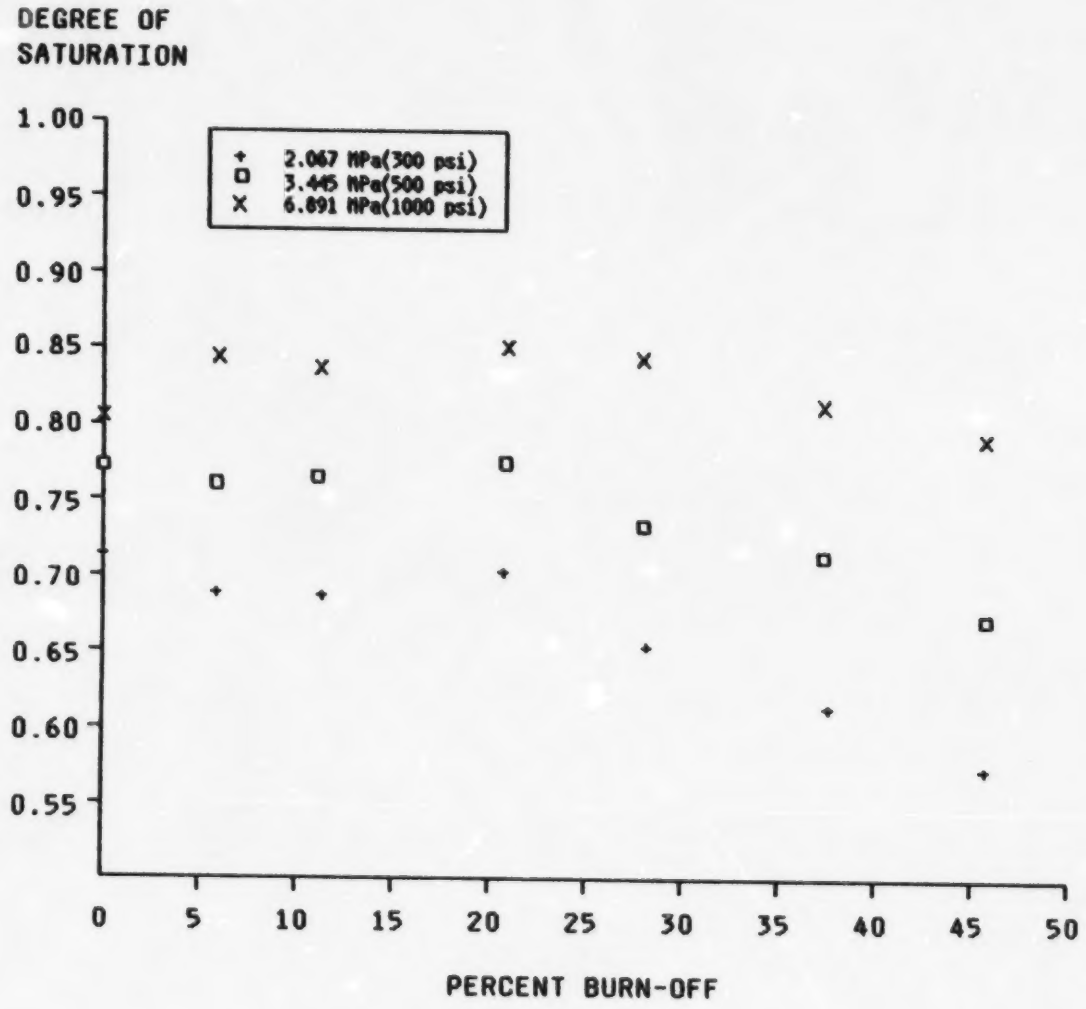

Figure 22/ Degree of Saturation, Calculated from Dubinin Plots

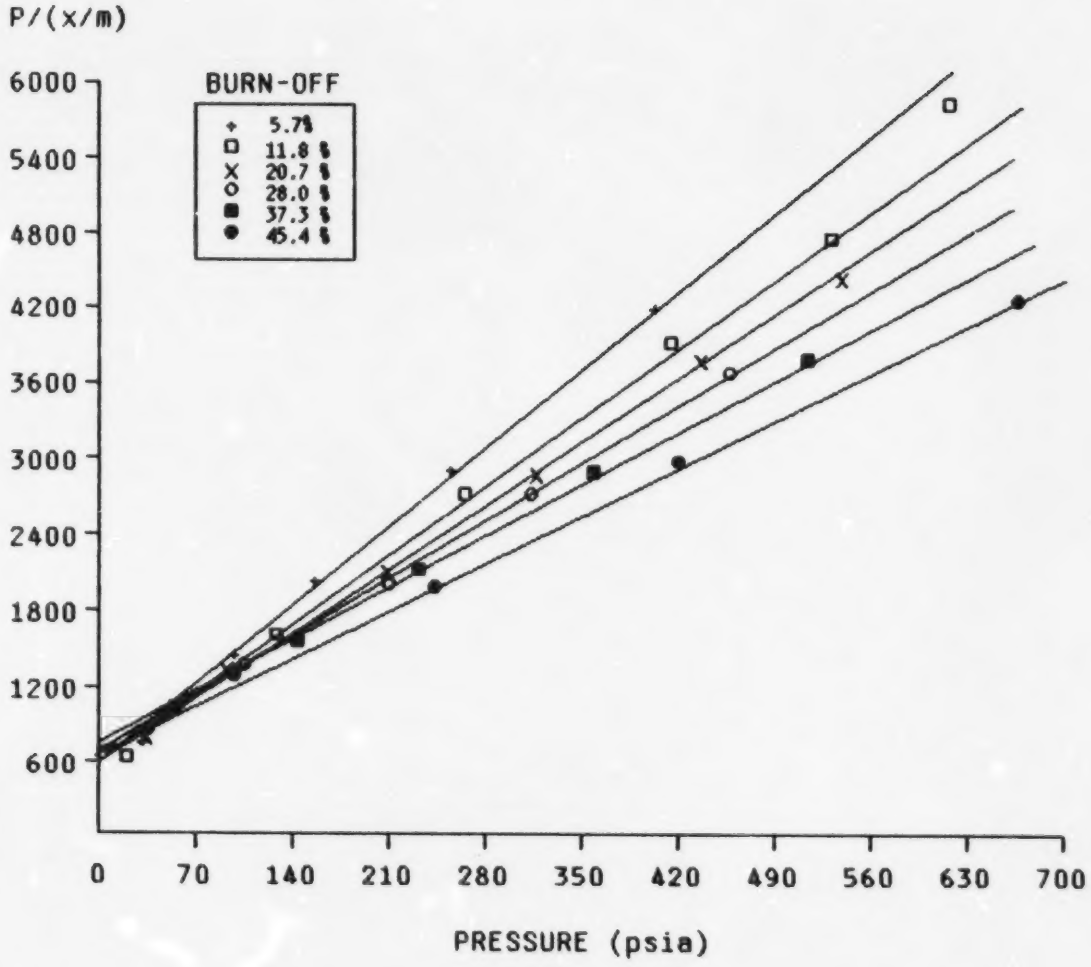

Figure 23/ Langmuir Plots -- Methane Isotherms, 25° C

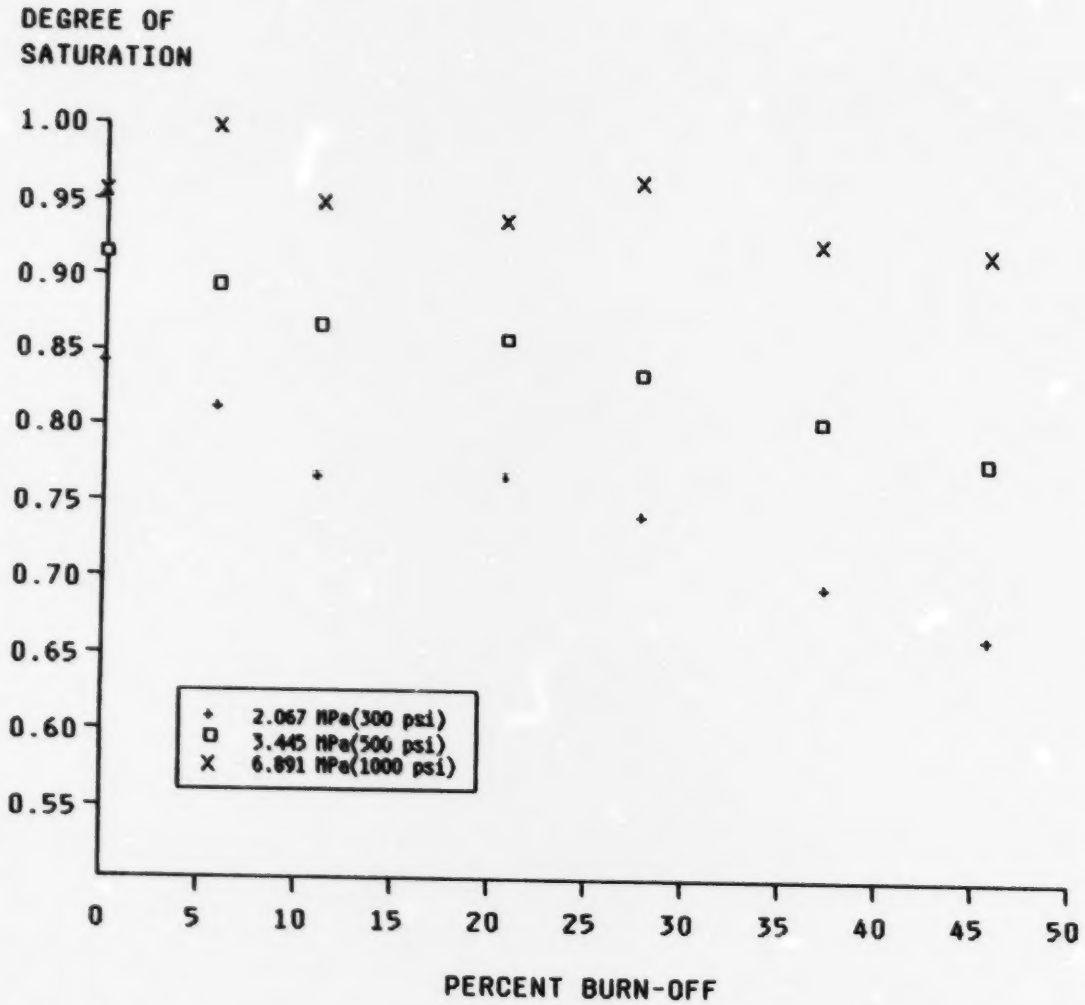

Figure 24/ Degree of Saturation, Calculated from Langmuir Plots

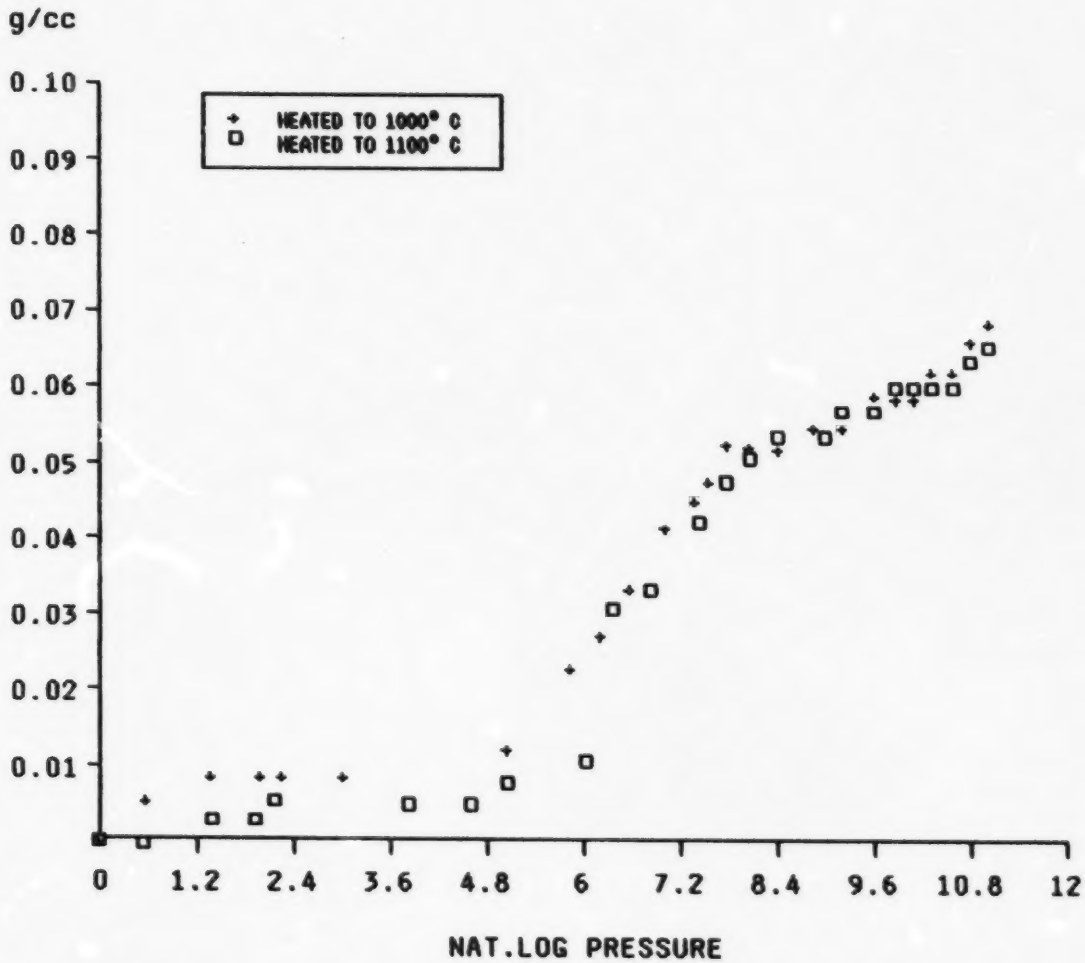

Figure 25/ Mercury Porosimetry -- Heat-Treated Saran Carbons

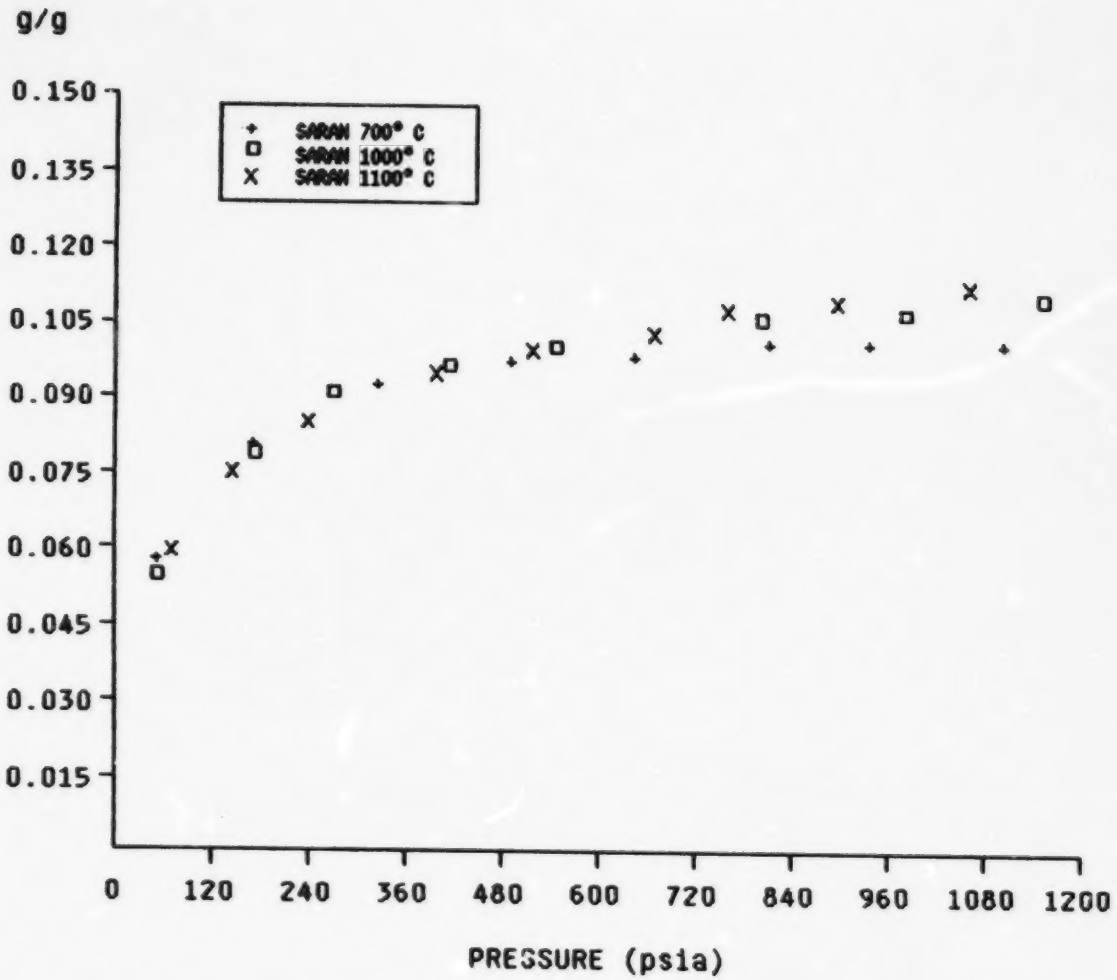

Figure 26/ Methane Adsorption -- Heat-Treated Saran Carbons